SIAM J. APPL. MATH.
Vol. 79, No. 4, pp. 1581–1606

TRAVEL FREQUENCY AND INFECTIOUS DISEASES*

DAOZHOU GAO†

Abstract. Empirical and statistical evidence suggests that the number of trips taken per year varies significantly among people by age, gender, income, occupation, ethnicity, region, and so on. Only a small fraction of people are frequent travelers while most travel occasionally or never. Taking the difference in travel frequency into consideration, we propose a multipatch epidemic model where humans in each patch are divided into susceptible unfrequent, infectious unfrequent, susceptible frequent, and infectious frequent classes. The basic reproduction number $\mathcal{R}_0$ is derived and shown to govern the global dynamics of the model system if infection does not impede travel. Lower and upper bounds on $\mathcal{R}_0$ are given, and the disease can become endemic or extinct even though it dies out or persists in each isolated patch. Both analytical and numerical approaches show that the model, without distinguishing the difference in travel frequency, tends to underestimate the infection risk. Several numerical examples are presented to illustrate the impact of changes in modern travel on disease spread. We find that $\mathcal{R}_0$ may decreasingly, or increasingly, or nonmonotonically depend on the diffusion coefficient of the infected subpopulation. Meanwhile, the basic reproduction number of the model with uniform travel frequency is shown to be monotone decreasing in the diffusion coefficient if the connectivity matrix is symmetric. The unfrequent travelers at high transmission regions are at the highest risk of infection, and allocating resources to frequent and unfrequent travelers in high transmission regions probably yields the maximal reduction in infections and the basic reproduction number, respectively.

Key words. travel frequency, patch model, multigroup, basic reproduction number, global dynamics, underestimate

AMS subject classifications. 92D30, 91D25, 34C60, 34D20, 37N25

DOI. 10.1137/18M1211957

1. Introduction.

Travel varies greatly over human history in distance (local, regional, national, and intercontinental), means (such as foot, horse, car, train, ship, and airplane), and purpose (such as business and recreation). Globalization, urbanization, and transport development have driven more people to move more frequently and farther at less cost of time and money. The number of road motor vehicles per 1,000 inhabitants in the U.S. reached 821 in 2015 [31]. The total length of high-speed rail in China has exceeded 31,000 km and will reach 38,000 km in 2025 [26]. The numbers of air passengers and international inbound tourists increased from 1.391 billion and 0.556 billion in 1996 to 3.705 billion and 1.235 billion in 2016 [40], respectively. These changes strengthen the connection between different economic entities but also facilitate the spread of common or novel infectious diseases, leading to a serious public health problem across the world. Influenza A (H1N1) was first reported in Mexico in March 2009 and spread to 168 countries and territories in late July 2009 [48]. The Zika virus disease hit Brazil in April 2015 and spread to much of South America, Central America, the Caribbean, and Mexico before it was contained [49]. On the other hand, human movement brings a big challenge to disease control and

*Received by the editors September 10, 2018; accepted for publication (in revised form) May 29, 2019; published electronically August 27, 2019.
https://doi.org/10.1137/18M1211957
Funding: This work was partially supported by the NSFC through grant 11601336, by the Program for Professor of Special Appointment (Eastern Scholar) at Shanghai Institutions of Higher Learning through grant TP2015050, and by the Shanghai Gaofeng Project for the University Academic Development Program.
†Department of Mathematics, Shanghai Normal University, Shanghai 200234, PR China (dzgao@shnu.edu.cn).

elimination. Over 98% (3,021 of 3,077) of malaria cases in China in 2014 are among travelers from Africa and southeast Asia [6].

Mathematical models have become an important tool in characterizing, predicting, and controlling the spatial and temporal spread of infectious diseases (see, for example, Arino [2], Gao and Ruan [20], and Wang [44]). With the development and application of new technologies, massive data (demography, epidemiology, travel, etc.) are available for checking the reliability and validity of modeling approaches so that a real-time large-scale disease surveillance system is gradually achievable. Bartlett [4] is among the first to propose a two-patch epidemic model with cross patch infection to explore the mechanism of recurrent epidemics. Dye and Hasibeder [12] and Hasibeder and Dye [22] considered a mosquito-borne disease model where a mosquito in any vector patch can bite in any host patch and showed that a heterogeneous mixing of vectors and hosts results in a higher basic reproduction number. Wang and Zhao [46] and Jin and Wang [28] analyzed an SIS patch model with mass-action incidence and found that the effect of population dispersal on disease spread is complicated. Cui, Takeuchi, and Saito [9] studied the influence of transport-related infection on disease dynamics. Wang et al. [47] formulated a multipatch SEIQR model to discuss the impact of entry-exit screening on disease control. Patch models are widely used to study specific infectious diseases including malaria [3, 8, 17, 19], rabies [7], cholera [13], bovine tuberculosis [14], Rift Valley fever [15, 50], influenza [24, 25, 33], West Nile virus [29, 51], and SARS [32].

However, these models disregard the difference in travel behavior by assuming that individuals in the same disease status have the same travel rate, which is inappropriate, for the distribution of travel frequency is typically uneven. Some people travel several times a month while some stay home or nearby for a whole year. For instance, the percentages of frequent air traveler, occasional air traveler, and never flown in the U.S. in 2015 are 7%, 71%, and 22%, respectively. A household survey in Norway found that 3.1% respondents who take domestic flights make more than 20 trips annually [10]. The travel frequency of an individual is determined by various factors such as occupation, age, gender, income, and residency, while the average frequency of a population is affected by development of public transit, possession of private vehicles, percentage of people with a driver's license, industry structure, and climatic condition. Jobs such as salesman, retail buyer, official, journalist, athlete, recruiter, consultant, pilot, and tour guide require travel frequently. In England, women make more trips but accumulate less mileage than men on average, the highest income households travel more than twice as far as the lowest, and rural residents travel around 44% farther than urban residents [37]. The National Household Travel Survey in the U.S. shows similar patterns [35]. It is worth mentioning that the importance of taking into account the effects of heterogeneity in travel frequency on the global spread of a directly transmitted disease was once addressed by Hollingsworth, Ferguson, and Anderson [23]. They used a stochastic SEIR model to simulate exportation of cases from an epidemic in a population for which a small proportion travel more frequently than the rest and concluded that infected people who travel often have the potential to spread infection even more rapidly.

The rest of this paper is organized as follows. In the next section, we develop a hybrid of metapopulation and multigroup models to highlight the difference in travel behaviors. In section 3, we derive the basic reproduction number which serves as a threshold for the disease extinction and persistence if the disease is not severe enough to impair mobility. Biologically meaningful estimates for the multipatch reproduction number are obtained. We compare our new model with previous models in terms of

the reproduction numbers. Three numerical examples are presented to illustrate the impact of changes in human movement on disease spread and the potential application of the model. The last section is devoted to a brief discussion of our main results and future work. We solve an open problem raised by Allen et al. [1] in the appendix.

2. Model formulation. We begin with an SIS model with standard incidence for the transmission of an infectious disease with population dispersal between p patches. In patch i, the population is divided into susceptible and infectious classes, with $S_i(t)$ and $I_i(t)$ denoting the number of susceptible and infectious individuals, respectively. Susceptible individuals contract the disease through contact with infectious individuals, and infectious individuals revert to susceptible class on recovery. Travelers migrate from one patch to another in a negligible period of time so that no infection or recovery takes place during travel. The dynamics of disease transmission in patch i are described by

$$\begin{aligned}\frac{dS_i}{dt} &= \varepsilon_i - \beta_i \frac{I_i}{N_i} S_i + \gamma_i I_i - \mu_i S_i + d_S \sum_{j=1}^{p} c_{ij} S_j, \quad 1 \le i \le p,\\ \frac{dI_i}{dt} &= \beta_i \frac{I_i}{N_i} S_i - (\gamma_i + \mu_i + \nu_i) I_i + d_I \sum_{j=1}^{p} d_{ij} I_j, \quad 1 \le i \le p,\end{aligned} \tag{2.1}$$

where $N_i = S_i + I_i$ represents the total population within a single patch, ε_i the recruitment rate due to newborns and immigrants, β_i the transmission coefficient, γ_i the recovery rate, μ_i the natural death rate, ν_i the disease-induced death rate, and d_S and d_I the respective diffusion coefficients for the susceptible and infected subpopulations. The parameters c_{ij} and d_{ij} denote, respectively, the degrees of movement for susceptible and infectious people from patch j to patch i for $i, j = 1, 2, \ldots, p$ and $i \neq j$, while $-c_{ii}$ and $-d_{ii}$ denote, respectively, the outgoing degrees of movement for susceptible and infectious people of patch i for $i = 1, 2, \ldots, p$. The ignorance of the death and birth processes during travel leads to

$$-c_{ii} = \sum_{j=1, j\neq i}^{p} c_{ji} \quad \text{and} \quad -d_{ii} = \sum_{j=1, j\neq i}^{p} d_{ji}, \quad i = 1, 2, \ldots, p.$$

The connectivity matrices $C = (c_{ij})_{p\times p}$ and $D = (d_{ij})_{p\times p}$ are assumed to be irreducible; otherwise the p patches can be split into multiple disconnected parts and studied separately.

The model (2.1) and its variant in a two-patch setting was intensively studied by Wang and Mulone [45], Salmani and van den Driesssche [34], and Sun et al. [38]. Later, Allen et al. [1] and Gao and Ruan [18] generalized these works to the model with an arbitrary number of patches. They established the threshold dynamics of the model in terms of the multipatch basic reproduction number. It was shown that the maximum and minimum of the set of the basic reproduction numbers of each isolated patch (i.e., no movement) are, respectively, the upper and lower bounds of the multipatch reproduction number. Epidemiologically, this implies that the disease persists or goes extinct in each isolated patch then remains persistent or extinct when all patches are connected by population dispersal. In particular, provided that the disease is non-fatal and susceptible and infectious individuals have the same connectivity

matrix, namely, the model (2.1) becomes

$$\begin{aligned}
\frac{dS_i}{dt} &= \varepsilon_i - \beta_i \frac{I_i}{N_i} S_i + \gamma_i I_i - \mu_i S_i + d_S \sum_{j=1}^{p} c_{ij} S_j, \quad 1 \le i \le p, \\
\frac{dI_i}{dt} &= \beta_i \frac{I_i}{N_i} S_i - (\gamma_i + \mu_i) I_i + d_I \sum_{j=1}^{p} c_{ij} I_j, \quad 1 \le i \le p,
\end{aligned} \tag{2.2}$$

then either the disease-free equilibrium or the endemic equilibrium is globally asymptomatically stable if $d_S \approx d_I$ [18].

We now consider the heterogeneity in travel frequency among individuals. For the sake of simplicity, only frequent and unfrequent travelers are introduced. A frequent traveler is a person who regularly makes more than a given number of long distance trips away from home per unit of time, e.g., six or more round trips of 50 miles or more a year. Based on disease status and travel behavior, the population in the ith patch is further divided into susceptible unfrequent, infectious unfrequent, susceptible frequent, and infectious frequent classes, denoted by S_i^u, I_i^u, S_i^f, and I_i^f, respectively. Thus the total population within patch i is $N_i = S_i^u + S_i^f + I_i^u + I_i^f$. We make some additional assumptions as follows:

(1) Individuals are recruited susceptible with a fraction θ_i being frequent.
(2) People do not change their travel frequency upon infection and recovery.
(3) Unfrequent and frequent people mutually transfer at constant rates, ϕ_i^u and ϕ_i^f, respectively, which are independent of disease status.
(4) Immigrants do not immediately change their travel frequency upon arrival at a new patch.
(5) The population within each patch is homogeneously mixed, but the transmission probability could vary from group to group.

The above assumptions and the flowchart shown in Figure 1 lead to a multigroup-multipatch epidemic model with consideration of travel difference ($1 \le i \le p$),

$$\begin{aligned}
\frac{dS_i^u}{dt} &= (1-\theta_i)\varepsilon_i - \lambda_i^u S_i^u + \gamma_i^u I_i^u - \mu_i^u S_i^u - \phi_i^u S_i^u + \phi_i^f S_i^f + d_S \sum_{j=1}^{p} c_{ij}^u S_j^u, \\
\frac{dS_i^f}{dt} &= \theta_i \varepsilon_i - \lambda_i^f S_i^f + \gamma_i^f I_i^f - \mu_i^f S_i^f + \phi_i^u S_i^u - \phi_i^f S_i^f + d_S \sum_{j=1}^{p} c_{ij}^f S_j^f, \\
\frac{dI_i^u}{dt} &= \lambda_i^u S_i^u - (\gamma_i^u + \mu_i^u) I_i^u - \phi_i^u I_i^u + \phi_i^f I_i^f + d_I \sum_{j=1}^{p} c_{ij}^u I_j^u, \\
\frac{dI_i^f}{dt} &= \lambda_i^f S_i^f - (\gamma_i^f + \mu_i^f) I_i^f + \phi_i^u I_i^u - \phi_i^f I_i^f + d_I \sum_{j=1}^{p} c_{ij}^f I_j^f,
\end{aligned} \tag{2.3}$$

where $\lambda_i^u = (\beta_i^{uu} I_i^u + \beta_i^{uf} I_i^f)/N_i$ and $\lambda_i^f = (\beta_i^{fu} I_i^u + \beta_i^{ff} I_i^f)/N_i$ are, respectively, the forces of infection for unfrequent and frequent travelers. Here $\beta_i^{uu}, \beta_i^{uf}, \beta_i^{fu}$, and β_i^{ff} denote, respectively, the transmission rates between classes S_i^u and I_i^u, S_i^u and I_i^f, S_i^f and I_i^u, and S_i^f and I_i^f. Other parameters have the same meaning as before with the superscripts u and f representing unfrequent and frequent classes, respectively. All

parameters are positive except $\theta_i \in [0,1]$ and the movement rates. Again, we have

$$-c_{ii}^u = \sum_{j=1, j\neq i}^{p} c_{ji}^u \quad \text{and} \quad -c_{ii}^f = \sum_{j=1, j\neq i}^{p} c_{ji}^f, \quad i = 1, 2, \ldots, p.$$

The addition of connectivity matrices for unfrequent and frequent travelers $C^u + C^f = (c_{ij}^u + c_{ij}^f)_{p\times p}$ is assumed to be irreducible. By definition, it is reasonable to require that $c_{ij}^u \leq c_{ij}^f$ for $i \neq j$, and an extreme case is that $C^u = 0$, i.e., the unfrequent travelers do not migrate between patches.

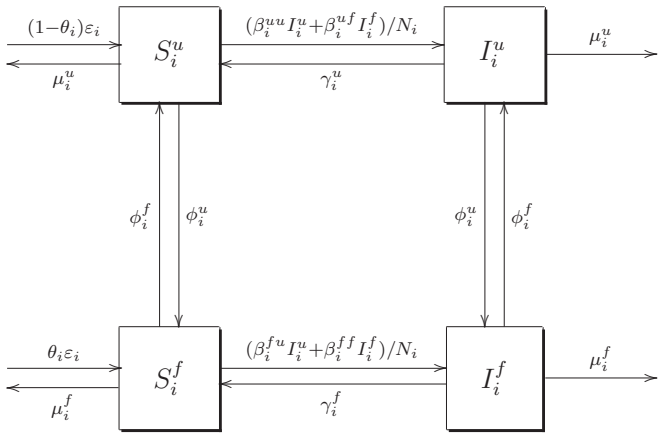

FIG. 1. *A schematic illustration of the two-group model for patch i omitting travel.*

Note that the multigroup model (2.3) cannot be regarded as a regular $2p$-patch model since I_i^f can infect S_i^u and I_i^u can infect S_i^f. The following result shows that the model system (2.3) is epidemiologically and mathematically well-posed.

THEOREM 2.1. *Solutions of system* (2.3) *with nonnegative initial conditions uniquely exist and remain nonnegative for all time $t \geq 0$. Moreover, the system is point dissipative.*

Proof. Define the incidence terms:

$$\beta_i^{uu} \frac{I_i^u}{N_i} S_i^u, \quad \beta_i^{uf} \frac{I_i^f}{N_i} S_i^u, \quad \beta_i^{fu} \frac{I_i^u}{N_i} S_i^f, \quad \text{and} \quad \beta_i^{ff} \frac{I_i^f}{N_i} S_i^f$$

equal zero whenever $N_i = 0$ for $i = 1, \ldots, p$. It is simple to verify that the vector field defined by the right-hand side of (2.3) is locally Lipschitz on $\mathbb{R}_+^{4p}$, so there exists a unique solution of system (2.3) for $t \geq 0$. The nonnegativity of each state variable can be directly verified via the corresponding model equation.

Let $\Lambda = \sum_{i=1}^p \varepsilon_i$ and $\Upsilon = \min\{\mu_1^u, \ldots, \mu_p^u, \mu_1^f, \ldots, \mu_p^f\}$. The total population over all patches, denoted by $N = \sum_{i=1}^p N_i$, satisfies

$$\frac{dN}{dt} = \sum_{i=1}^{p} \left(\varepsilon_i - \mu_i^u N_i^u - \mu_i^f N_i^f \right) \leq \Lambda - \Upsilon N,$$

which implies $N(t)$ is bounded above by Λ/Υ for sufficiently large t. ∎

3. Mathematical analysis. In this section, we first study the existence and uniqueness of the disease-free equilibrium, define the basic reproduction number, and give its estimation. Then we investigate the disease dynamics of the system. Second, we consider the single patch case and estimate the proportion of residents who travel frequently. At the end we perform a comparative study between the traditional model (2.2) and the new model (2.3).

3.1. Disease-free equilibrium and reproductive number. In the absence of disease, the numbers of unfrequent and frequent travelers in patch i, denoted, respectively, by $N_i^u = S_i^u + I_i^u$ and $N_i^f = S_i^f + I_i^f$, satisfy

$$\begin{aligned}
\frac{dN_i^u}{dt} &= (1-\theta_i)\varepsilon_i - \mu_i^u N_i^u - \phi_i^u N_i^u + \phi_i^f N_i^f + d_S \sum_{j=1}^{p} c_{ij}^u N_j^u, \quad 1 \le i \le p, \\
\frac{dN_i^f}{dt} &= \theta_i \varepsilon_i - \mu_i^f N_i^f + \phi_i^u N_i^u - \phi_i^f N_i^f + d_S \sum_{j=1}^{p} c_{ij}^f N_j^f, \quad 1 \le i \le p.
\end{aligned} \tag{3.1}$$

It follows from the irreducibility of the matrix $C^u + C^f$ that the coefficient matrix of the equilibrium equations

$$\begin{aligned}
(\mu_i^u + \phi_i^u) N_i^u - \phi_i^f N_i^f - d_S \sum_{j=1}^{p} c_{ij}^u N_j^u &= (1-\theta_i)\varepsilon_i, \quad 1 \le i \le p, \\
-\phi_i^u N_i^u + (\mu_i^f + \phi_i^f) N_i^f - d_S \sum_{j=1}^{p} c_{ij}^f N_j^f &= \theta_i \varepsilon_i, \quad 1 \le i \le p,
\end{aligned} \tag{3.2}$$

or explicitly

$$A = \begin{pmatrix} A_{11} & -A_{12} \\ -A_{21} & A_{22} \end{pmatrix},$$

is irreducible with $A_{11} = \operatorname{diag}\{\mu_1^u + \phi_1^u, \dots, \mu_p^u + \phi_p^u\} - d_S C^u$, $A_{12} = \operatorname{diag}\{\phi_1^f, \dots, \phi_p^f\}$, $A_{21} = \operatorname{diag}\{\phi_1^u, \dots, \phi_p^u\}$, and $A_{22} = \operatorname{diag}\{\mu_1^f + \phi_1^f, \dots, \mu_p^f + \phi_p^f\} - d_S C^f$. Thus A is a nonsingular M-matrix with positive inverse and hence (3.2) has a unique solution $(\boldsymbol{N}^{u*}, \boldsymbol{N}^{f*})$ with $\boldsymbol{N}^{u*} = (N_1^{u*}, \dots, N_p^{u*}) \gg \mathbf{0}$ and $\boldsymbol{N}^{f*} = (N_1^{f*}, \dots, N_p^{f*}) \gg \mathbf{0}$. So the model (2.3) has a unique disease-free equilibrium $E_0 = (\boldsymbol{N}^{u*}, \boldsymbol{N}^{f*}, \mathbf{0}, \mathbf{0})$, where $\mathbf{0}$ is a zero row vector with p entries.

Using the next generation operator approach as described by Diekmann, Heesterbeek, and Metz [11] and the recipe of van den Driessche and Watmough [43], the new infection and transition matrices are, respectively, given by

$$F = \begin{pmatrix} F_{11} & F_{12} \\ F_{21} & F_{22} \end{pmatrix} \quad \text{and} \quad V = \begin{pmatrix} V_{11} & -V_{12} \\ -V_{21} & V_{22} \end{pmatrix}$$

with

$$\begin{aligned}
F_{11} &= \operatorname{diag}\left\{\beta_1^{uu} \frac{N_1^{u*}}{N_1^*}, \dots, \beta_p^{uu} \frac{N_p^{u*}}{N_p^*}\right\}, \quad F_{12} = \operatorname{diag}\left\{\beta_1^{uf} \frac{N_1^{u*}}{N_1^*}, \dots, \beta_p^{uf} \frac{N_p^{u*}}{N_p^*}\right\}, \\
F_{21} &= \operatorname{diag}\left\{\beta_1^{fu} \frac{N_1^{f*}}{N_1^*}, \dots, \beta_p^{fu} \frac{N_p^{f*}}{N_p^*}\right\}, \quad F_{22} = \operatorname{diag}\left\{\beta_1^{ff} \frac{N_1^{f*}}{N_1^*}, \dots, \beta_p^{ff} \frac{N_p^{f*}}{N_p^*}\right\},
\end{aligned}$$

and

$$V_{11} = \mathrm{diag}\{\gamma_1^u + \mu_1^u + \phi_1^u, \ldots, \gamma_p^u + \mu_p^u + \phi_p^u\} - d_I C^u, \quad V_{12} = \mathrm{diag}\{\phi_1^f, \ldots, \phi_p^f\},$$
$$V_{21} = \mathrm{diag}\{\phi_1^u, \ldots, \phi_p^u\}, \quad V_{22} = \mathrm{diag}\{\gamma_1^f + \mu_1^f + \phi_1^f, \ldots, \gamma_p^f + \mu_p^f + \phi_p^f\} - d_I C^f.$$

The basic reproduction number of model (2.3) is defined as the spectral radius of the next generation matrix FV^{-1}, that is,

$$\mathcal{R}_0 = \rho(FV^{-1}).$$

Note that $\mathcal{R}_0$ depends on all model parameters. In particular, $\mathcal{R}_0$ constantly increases in transmission rates $\beta_i^{uu}, \beta_i^{uf}, \beta_i^{fu}$, and β_i^{ff}, but decreases in recovery rates γ_i^u and γ_i^f. The dependence of $\mathcal{R}_0$ on other parameters is more complicated and will be explored later in a numerical way. The inverse of the two-by-two block matrix V is

$$V^{-1} = \begin{pmatrix} (V_{11} - V_{12}V_{22}^{-1}V_{21})^{-1} & V_{11}^{-1}V_{12}(V_{22} - V_{21}V_{11}^{-1}V_{12})^{-1} \\ V_{22}^{-1}V_{21}(V_{11} - V_{12}V_{22}^{-1}V_{21})^{-1} & (V_{22} - V_{21}V_{11}^{-1}V_{12})^{-1} \end{pmatrix}.$$

Denoting the diagonal blocks of V^{-1} by V_{11}^* and V_{22}^*, the matrix FV^{-1} takes the form

$$\begin{pmatrix} (F_{11} + F_{12}V_{22}^{-1}V_{21})V_{11}^* & (F_{11}V_{11}^{-1}V_{12} + F_{12})V_{22}^* \\ (F_{21} + F_{22}V_{22}^{-1}V_{21})V_{11}^* & (F_{21}V_{11}^{-1}V_{12} + F_{22})V_{22}^* \end{pmatrix}.$$

However, it is generally difficult to solve $\mathcal{R}_0$ explicitly and write it concisely in terms of model parameters even for the two-patch case. Hence, some mathematically tractable and biologically meaningful bounds on the value of $\mathcal{R}_0$ are desirable [2, 18, 24].

THEOREM 3.1. *Define*

$$\mathcal{R}_i^{uu} = \frac{\beta_i^{uu}}{\gamma_i^u + \mu_i^u}, \quad \mathcal{R}_i^{uf} = \frac{\beta_i^{uf}}{\gamma_i^f + \mu_i^f}, \quad \mathcal{R}_i^{fu} = \frac{\beta_i^{fu}}{\gamma_i^u + \mu_i^u}, \quad \mathcal{R}_i^{ff} = \frac{\beta_i^{ff}}{\gamma_i^f + \mu_i^f}$$

as the average number of secondary cases produced by a typical unfrequent/frequent traveler in a completely unfrequent/frequent susceptible population during the entire infection period of the person. For system (2.3)*, the inequality*

$$\min_{1\le i\le p}\left\{\mathcal{R}_i^{uu}, \mathcal{R}_i^{uf}, \mathcal{R}_i^{fu}, \mathcal{R}_i^{ff}\right\} \le \mathcal{R}_0 \le \max_{1\le i\le p}\left\{\mathcal{R}_i^{uu}, \mathcal{R}_i^{uf}, \mathcal{R}_i^{fu}, \mathcal{R}_i^{ff}\right\}$$

holds.

Proof. Without loss of generality, we assume that

$$\mathcal{R}_1^{uu} = \min_{1\le i\le p}\left\{\mathcal{R}_i^{uu}, \mathcal{R}_i^{uf}, \mathcal{R}_i^{fu}, \mathcal{R}_i^{ff}\right\} \quad \text{and} \quad \mathcal{R}_p^{ff} = \max_{1\le i\le p}\left\{\mathcal{R}_i^{uu}, \mathcal{R}_i^{uf}, \mathcal{R}_i^{fu}, \mathcal{R}_i^{ff}\right\}.$$

Let $\alpha_i^u = \gamma_i^u + \mu_i^u$ and $\alpha_i^f = \gamma_i^f + \mu_i^f$ for $1 \le i \le p$ and

$$\tilde{F}_{11} = \mathrm{diag}\left\{\alpha_1^u \frac{N_1^{u*}}{N_1^*}, \ldots, \alpha_p^u \frac{N_p^{u*}}{N_p^*}\right\}, \quad \tilde{F}_{12} = \mathrm{diag}\left\{\alpha_1^f \frac{N_1^{u*}}{N_1^*}, \ldots, \alpha_p^f \frac{N_p^{u*}}{N_p^*}\right\},$$
$$\tilde{F}_{21} = \mathrm{diag}\left\{\alpha_1^u \frac{N_1^{f*}}{N_1^*}, \ldots, \alpha_p^u \frac{N_p^{f*}}{N_p^*}\right\}, \quad \tilde{F}_{22} = \mathrm{diag}\left\{\alpha_1^f \frac{N_1^{f*}}{N_1^*}, \ldots, \alpha_p^f \frac{N_p^{f*}}{N_p^*}\right\}.$$

It follows from

$$\hat{F} := \mathcal{R}_1^{uu} \begin{pmatrix} \tilde{F}_{11} & \tilde{F}_{12} \\ \tilde{F}_{21} & \tilde{F}_{22} \end{pmatrix} \le F = \begin{pmatrix} F_{11} & F_{12} \\ F_{21} & F_{22} \end{pmatrix} \le \tilde{F} := \mathcal{R}_p^{ff} \begin{pmatrix} \tilde{F}_{11} & \tilde{F}_{12} \\ \tilde{F}_{21} & \tilde{F}_{22} \end{pmatrix}$$

and

$$(1, \dots, 1)\hat{F} = \mathcal{R}_1^{uu}(\alpha_1^u, \dots, \alpha_p^u, \alpha_1^f, \dots, \alpha_p^f) = \mathcal{R}_1^{uu}(1, \dots, 1)V,$$
$$(1, \dots, 1)\tilde{F} = \mathcal{R}_p^{ff}(\alpha_1^u, \dots, \alpha_p^u, \alpha_1^f, \dots, \alpha_p^f) = \mathcal{R}_p^{ff}(1, \dots, 1)V$$

that $\hat{F}V^{-1} \le FV^{-1} \le \tilde{F}V^{-1}$ and $\rho(\hat{F}V^{-1}) = \mathcal{R}_1^{uu}, \rho(\tilde{F}V^{-1}) = \mathcal{R}_p^{ff}$. So, $\rho(\hat{F}V^{-1}) = \mathcal{R}_1^{uu} \le \mathcal{R}_0 = \rho(FV^{-1}) \le \rho(\tilde{F}V^{-1}) = \mathcal{R}_p^{ff}$. ∎

3.2. Threshold dynamics. It follows from Theorem 2 in van den Driessche and Watmough [43] that the disease-free equilibrium E_0 of system (2.3) is locally asymptotically stable if $\mathcal{R}_0 < 1$ and unstable otherwise. Furthermore, similar to the proof of Theorem 2.5 in Gao and Ruan [18], we can use the persistence theory [52] to show the uniform persistence of the disease and the existence of at least one endemic equilibrium when $\mathcal{R}_0 > 1$. In particular, the global dynamics of the model system are completely governed by the reproductive number as population dispersal is unaffected by the disease by applying the theory of monotone dynamical systems [27, 36, 52].

THEOREM 3.2. *For model* (2.3) *with* $d_S = d_I$*, the disease-free equilibrium* E_0 *is globally asymptotically stable on the nonnegative orthant* $\mathbb{R}_+^{4p}$ *if* $\mathcal{R}_0 \le 1$*, and there is a unique endemic equilibrium* $E^* = (\boldsymbol{S}^{u*}, \boldsymbol{S}^{f*}, \boldsymbol{I}^{u*}, \boldsymbol{I}^{f*})$ *which is globally asymptotically stable on the nonnegative orthant minus the set of all disease-free states if* $\mathcal{R}_0 > 1$*.*

Proof. Since the coefficient matrix of the linear system (3.1), i.e., $-A$, is strictly diagonally dominant, by the Gershgorin circle theorem, all eigenvalues of $-A$ have negative real parts. Hence the equilibrium $(\boldsymbol{N}^{u*}, \boldsymbol{N}^{f*})$ of system (3.1) is globally asymptotically stable on $\mathbb{R}_+^{2p}$. Since $N_i^u(t) \to N_i^{u*}$ and $N_i^f(t) \to N_i^{f*}$ as $t \to \infty$ for $i = 1, \dots, p$, system (2.3) gives the limiting system ($1 \le i \le p$):

$$\begin{aligned} \frac{dI_i^u}{dt} &= \lambda_i^{u*}(N_i^{u*} - I_i^u) - (\gamma_i^u + \mu_i^u)I_i^u - \phi_i^u I_i^u + \phi_i^f I_i^f + d_I \sum_{j=1}^{p} c_{ij}^u I_j^u, \\ \frac{dI_i^f}{dt} &= \lambda_i^{f*}(N_i^{f*} - I_i^f) - (\gamma_i^f + \mu_i^f)I_i^f + \phi_i^u I_i^u - \phi_i^f I_i^f + d_I \sum_{j=1}^{p} c_{ij}^f I_j^f, \end{aligned} \tag{3.3}$$

where $\lambda_i^{u*} = (\beta_i^{uu} I_i^u + \beta_i^{uf} I_i^f)/N_i^*$ and $\lambda_i^{f*} = (\beta_i^{fu} I_i^u + \beta_i^{ff} I_i^f)/N_i^*$.

Let h be the vector field described by (3.3), with ψ_t the corresponding flow. Obviously, system (3.3) is cooperative and irreducible on the order interval

$$\mathbb{D} = \{(I_1^u, \dots, I_p^u, I_1^f, \dots, I_p^f) \in \mathbb{R}_+^{2p} : 0 \le I_i^u \le N_i^{u*}, 0 \le I_i^f \le N_i^{f*}, i = 1, \dots, p\}.$$

For any $\alpha \in (0, 1)$ and any $\boldsymbol{x} = (I_1^u, \dots, I_p^u, I_1^f, \dots, I_p^f) \in \mathbb{D}$ with $\boldsymbol{x} \gg \boldsymbol{0}$, the fact

$$h_i(\alpha \boldsymbol{x}) - \alpha h_i(\boldsymbol{x}) = \begin{cases} \alpha(1-\alpha)\lambda_i^{u*} I_i^u > 0, & i = 1, \dots, p, \\ \alpha(1-\alpha)\lambda_i^{f*} I_i^f > 0, & i = p+1, \dots, 2p, \end{cases}$$

implies that h is strongly sublinear on $\mathbb{D}$. In addition, the set $\mathbb{D}$ is positively invariant with respect to (3.3) due to $h_i(\boldsymbol{x}) \ge 0$ for $\boldsymbol{x} \in \mathbb{D}$ with $x_i = 0$, $i = 1, \dots, 2p$, and $h_i(\boldsymbol{x}) \le 0$ for $\boldsymbol{x} \in \mathbb{D}$ with $x_i = N_i^{u*}$, $i = 1, \dots, p$, and $x_i = N_i^{f*}$, $i = p+1, \dots, 2p$.

The proof of Theorem 2 in van den Driessche and Watmough [43] indicates that $s(Dh(\mathbf{0})) = s(F-V) \le 0 \Leftrightarrow \mathcal{R}_0 = \rho(FV^{-1}) \le 1$ and $s(Dh(\mathbf{0})) > 0 \Leftrightarrow \mathcal{R}_0 > 1$. By Corollary 3.2 in Zhao and Jing [53] or Theorem 2.3.4 in Zhao [52], if $\mathcal{R}_0 \le 1$, then $\boldsymbol{x} = \mathbf{0}$ is globally asymptotically stable with respect to $\mathbb{D}$, and if $\mathcal{R}_0 > 1$, then (3.3) admits a unique positive equilibrium $\boldsymbol{x}^* = (\boldsymbol{I}^{u*}, \boldsymbol{I}^{f*}) \in \mathbb{D}$, which is globally asymptotically stable with respect to $\mathbb{D}\backslash\{\mathbf{0}\}$.

The strong monotonicity of ψ_t on $\mathbb{D}$ implies that $(\boldsymbol{I}^{u*}, \boldsymbol{I}^{f*}) \ll (\boldsymbol{N}^{u*}, \boldsymbol{N}^{f*})$, or equivalently, $(\boldsymbol{S}^{u*}, \boldsymbol{S}^{f*}) = (\boldsymbol{N}^{u*} - \boldsymbol{I}^{u*}, \boldsymbol{N}^{f*} - \boldsymbol{I}^{f*}) \gg \mathbf{0}$. Thus (2.3) has a unique endemic equilibrium $E^* = (S_1^*, S_2^*, \dots, S_p^*, I_1^*, I_2^*, \dots, I_p^*)$ provided that $\mathcal{R}_0 > 1$. With the application of the theory of asymptotically autonomous systems or internally chain transitive sets [5, 17, 52], the conclusion of the theorem follows. ∎

3.3. Single patch model. In the case where human movement disappears or only one patch is considered, the transmission dynamics of a given patch are described by the following differential equations:

$$
\begin{aligned}
\frac{dS_i^u}{dt} &= (1-\theta_i)\varepsilon_i - (\beta_i^{uu} I_i^u + \beta_i^{uf} I_i^f)\frac{S_i^u}{N_i} + \gamma_i^u I_i^u - \mu_i^u S_i^u - \phi_i^u S_i^u + \phi_i^f S_i^f,\\
\frac{dS_i^f}{dt} &= \theta_i\varepsilon_i - (\beta_i^{fu} I_i^u + \beta_i^{ff} I_i^f)\frac{S_i^f}{N_i} + \gamma_i^f I_i^f - \mu_i^f S_i^f + \phi_i^u S_i^u - \phi_i^f S_i^f,\\
\frac{dI_i^u}{dt} &= (\beta_i^{uu} I_i^u + \beta_i^{uf} I_i^f)\frac{S_i^u}{N_i} - (\gamma_i^u + \mu_i^u) I_i^u - \phi_i^u I_i^u + \phi_i^f I_i^f,\\
\frac{dI_i^f}{dt} &= (\beta_i^{fu} I_i^u + \beta_i^{ff} I_i^f)\frac{S_i^f}{N_i} - (\gamma_i^f + \mu_i^f) I_i^f + \phi_i^u I_i^u - \phi_i^f I_i^f.
\end{aligned}
\tag{3.4}
$$

Direct calculation yields the disease-free equilibrium of the above system,

$$
E_0^{(i)} = (N_i^{u*}, N_i^{f*}, 0, 0) = \frac{\varepsilon_i}{\Delta_i}\left((1-\theta_i)\mu_i^f + \phi_i^f, \theta_i\mu_i^u + \phi_i^u, 0, 0\right),
$$

where $\Delta_i = (\mu_i^u + \phi_i^u)(\mu_i^f + \phi_i^f) - \phi_i^u\phi_i^f > 0$. Let $N_i^* = N_i^{u*} + N_i^{f*}$. The basic reproduction number of patch i in isolation is

$$
\mathcal{R}_0^{(i)} = \rho(F_i V_i^{-1}),
$$

where

$$
F_i = \frac{1}{N_i^*}\begin{pmatrix} \beta_i^{uu} N_i^{u*} & \beta_i^{uf} N_i^{u*} \\ \beta_i^{fu} N_i^{f*} & \beta_i^{ff} N_i^{f*} \end{pmatrix} \quad \text{and} \quad V_i = \begin{pmatrix} \gamma_i^u + \mu_i^u + \phi_i^u & -\phi_i^f \\ -\phi_i^u & \gamma_i^f + \mu_i^f + \phi_i^f \end{pmatrix}.
$$

Note that F_i is independent of ε_i, and so is $\mathcal{R}_0^{(i)}$. The single patch reproduction number $\mathcal{R}_0^{(i)}$ is explicitly solvable, but in a rather complicated form. The radical sign in $\mathcal{R}_0^{(i)}$ can be removed if $\beta_i^{uu} = \beta_i^{fu}$ and $\beta_i^{uf} = \beta_i^{ff}$. Particularly, $\mathcal{R}_0^{(i)}$ equals $\beta_i/(\gamma_i + \mu_i)$ for any $\phi_i^u > 0$ and $\phi_i^f > 0$ in a homogeneous setting: $\beta_i^{uu} = \beta_i^{uf} = \beta_i^{fu} = \beta_i^{ff} = \beta_i, \gamma_i^u = \gamma_i^f = \gamma_i$ and $\mu_i^u = \mu_i^f = \mu_i$.

We can similarly establish the estimation of the lower and upper bounds on $\mathcal{R}_0^{(i)}$.

COROLLARY 3.3. *For system* (3.4)*, the inequality*

$$
\min\left\{\mathcal{R}_i^{uu}, \mathcal{R}_i^{uf}, \mathcal{R}_i^{fu}, \mathcal{R}_i^{ff}\right\} \le \mathcal{R}_0^{(i)} \le \max\left\{\mathcal{R}_i^{uu}, \mathcal{R}_i^{uf}, \mathcal{R}_i^{fu}, \mathcal{R}_i^{ff}\right\}
$$

holds.

Again by the theory of monotone dynamical systems [36] and asymptotically autonomous systems [5], we obtain a threshold dynamics result.

COROLLARY 3.4. *For single patch model* (3.4)*, the disease-free equilibrium* $E_0^{(i)}$ *is globally asymptotically stable on* $\mathbb{R}^4_+$ *if* $\mathcal{R}_0^{(i)} \le 1$*, and the endemic equilibrium* $E_i^* = (S_i^{u*}, S_i^{f*}, I_i^{u*}, I_i^{f*})$ *exists and is globally asymptotically stable on* $\mathbb{R}^4_+$ *minus the set of all disease-free states if* $\mathcal{R}_0^{(i)} > 1$.

Remark 3.5. In the absence of population dispersal and disease, the fraction of frequent travelers with patch i converges to

$$\frac{N_i^{f*}}{N_i^{u*}+N_i^{f*}} = \frac{\phi_i^u + \theta_i\mu_i^u}{\phi_i^u + \phi_i^f + \theta_i\mu_i^u + (1-\theta_i)\mu_i^f} \approx \frac{\phi_i^u}{\phi_i^u+\phi_i^f},$$

when μ_i^u and μ_i^f are relatively small. When travelers disperse between patches, by the first equation of (3.1) at the equilibrium $(\boldsymbol{N}^{u*}, \boldsymbol{N}^{f*})$, the fraction also tends to

$$\begin{aligned}\frac{N_i^{f*}}{N_i^{u*}+N_i^{f*}} =& 1 - \frac{\phi_i^f N_i^{u*}}{\phi_i^f N_i^{u*} - ((1-\theta_i)\varepsilon_i - (\mu_i^u+\phi_i^u)N_i^{u*} + d_S\sum_j c_{ij}^u N_j^{u*})} \\ =& 1 - \frac{\phi_i^f}{\phi_i^f + \phi_i^u - ((1-\theta_i)\varepsilon_i - \mu_i^u N_i^{u*} + d_S\sum_j c_{ij}^u N_j^{u*})/N_i^{u*}} \approx \frac{\phi_i^u}{\phi_i^u+\phi_i^f}\end{aligned}$$

if the per capita change rate of the population of unfrequent travelers is small.

Roughly speaking, the fraction of frequent travelers of the ith patch is primarily determined by the frequency exchange rates ϕ_i^u and ϕ_i^f. Moreover, both the size and fraction of frequent travelers of patch i at the disease-free equilibrium are increasing in ϕ_i^u but decreasing in ϕ_i^f by applying the following result to (3.2), which can be viewed as a simple $2p$-patch population model. Symmetrically, both the size and fraction of unfrequent travelers of patch i are decreasing in ϕ_i^u but increasing in ϕ_i^f.

PROPOSITION 3.6. *Consider a single species population model,*

$$\frac{dN_i}{dt} = \varepsilon_i - \mu_i N_i + \sum_{j=1}^p c_{ij}N_j, \quad 1 \le i \le p,$$

where $(\varepsilon_1, \dots, \varepsilon_p) > 0$ *and* $(\mu_1, \dots, \mu_p) \gg 0$*, and* $C = (c_{ij})$ *is an irreducible and quasi-positive matrix with zero column sums. Then there exists a unique positive equilibrium* $\boldsymbol{N}^* = (N_1^*, \dots, N_p^*)$ *which is globally asymptotically stable on the nonnegative orthant. Furthermore, we have*

$$\frac{\partial N_i^*}{\partial c_{ij}} > 0 \quad \textit{and} \quad \frac{\partial N_j^*}{\partial c_{ij}} < 0$$

for $i, j = 1, \dots, p$ *and* $i \ne j$.

Proof. The first part follows from the argument on the equilibrium solution of (3.1). Without loss of generality we only consider $\partial N_1^*/\partial c_{21}$ and $\partial N_2^*/\partial c_{21}$. Since $\boldsymbol{N}^*$ is the solution of the linear equations

$$\varepsilon_i - \mu_i N_i^* + \sum_{j=1}^p c_{ij}N_j^* = 0, \quad 1 \le i \le p, \tag{3.5}$$

it follows from the implicit function theorem that $\partial N_i^*/\partial c_{21}$ exists for $i = 1, \ldots, p$. Differentiating (3.5) with respect to c_{21} yields

$$B\left(\frac{\partial N_1^*}{\partial c_{21}}, \frac{\partial N_2^*}{\partial c_{21}}, \frac{\partial N_3^*}{\partial c_{21}}, \ldots, \frac{\partial N_p^*}{\partial c_{21}}\right)^T = (-N_1^*, N_1^*, 0, \ldots, 0)^T$$

with $B = \mathrm{diag}\{\mu_1, \ldots, \mu_p\} - C$ a diagonally dominant matrix. Note that B has a positive inverse $B^{-1} = B^*/|B|$ with B^* and $|B|$ denoting the adjoint matrix and the determinant of B, respectively. Thus,

$$\begin{pmatrix} \frac{\partial N_1^*}{\partial c_{21}} & \frac{\partial N_2^*}{\partial c_{21}} \end{pmatrix}^T = \frac{1}{|B|}\begin{pmatrix} b_{11} & -b_{21} \\ -b_{12} & b_{22} \end{pmatrix}\begin{pmatrix} -N_1^* \\ N_1^* \end{pmatrix} = \frac{N_1^*}{|B|}\begin{pmatrix} -b_{11} - b_{21} \\ b_{12} + b_{22} \end{pmatrix},$$

where

$$b_{11} = \begin{vmatrix} \mu_2 - c_{22} & -c_{23} & \cdots & -c_{2p} \\ -c_{32} & \mu_3 - c_{33} & \cdots & -c_{3p} \\ \vdots & \vdots & \ddots & \vdots \\ -c_{p2} & -c_{p3} & \cdots & \mu_p - c_{pp} \end{vmatrix},$$

$$b_{21} = \begin{vmatrix} -c_{12} & -c_{13} & \cdots & -c_{1p} \\ -c_{32} & \mu_3 - c_{33} & \cdots & -c_{3p} \\ \vdots & \vdots & \ddots & \vdots \\ -c_{p2} & -c_{p3} & \cdots & \mu_p - c_{pp} \end{vmatrix},$$

$$b_{22} = \begin{vmatrix} \mu_1 - c_{11} & -c_{13} & \cdots & -c_{1p} \\ -c_{31} & \mu_3 - c_{33} & \cdots & -c_{3p} \\ \vdots & \vdots & \ddots & \vdots \\ -c_{p1} & -c_{p3} & \cdots & \mu_p - c_{pp} \end{vmatrix},$$

$$b_{12} = \begin{vmatrix} -c_{21} & -c_{23} & \cdots & -c_{2p} \\ -c_{31} & \mu_3 - c_{33} & \cdots & -c_{3p} \\ \vdots & \vdots & \ddots & \vdots \\ -c_{p1} & -c_{p3} & \cdots & \mu_p - c_{pp} \end{vmatrix}.$$

Hence,

$$b_{11} + b_{21} = \begin{vmatrix} \mu_2 - c_{22} - c_{12} & -c_{23} - c_{13} & \cdots & -c_{2p} - c_{1p} \\ -c_{32} & \mu_3 - c_{33} & \cdots & -c_{3p} \\ \vdots & \vdots & \ddots & \vdots \\ -c_{p2} & -c_{p3} & \cdots & \mu_p - c_{pp} \end{vmatrix} > 0,$$

$$b_{12} + b_{22} = \begin{vmatrix} \mu_1 - c_{11} - c_{21} & -c_{13} - c_{23} & \cdots & -c_{1p} - c_{2p} \\ -c_{31} & \mu_3 - c_{33} & \cdots & -c_{3p} \\ \vdots & \vdots & \ddots & \vdots \\ -c_{p1} & -c_{p3} & \cdots & \mu_p - c_{pp} \end{vmatrix} > 0.$$

The last step follows from the Gershgorin circle theorem. ∎

Remark 3.7. When three or more patches are concerned, the impact of increasing movement from patch j to patch i on the population size of patch k is uncertain with distinct i, j, k. In fact, the population size of patch k at the positive equilibrium, N_k^*, could be increasing or decreasing or even nonmonotonic in c_{ij}. The above proposition fails if the population growth model of each patch in isolation is changed to the logistic model.

3.4. Traditional model versus new model. To compare the traditional model (2.2) with the new model (2.3) in terms of their respective basic reproduction numbers, we put them on the same baseline from a biological and epidemiological perspective. Suppose all parameter values of the new model are given and those of the traditional model are to be determined. First, the two models are used to describe the same patchy environment, so their numbers of within-patch residents and between-patch travelers must be consistent at their disease-free equilibria. The numbers of unfrequent and frequent residents of the new model are given by the unique equilibrium $(\boldsymbol{N}^{u*}, \boldsymbol{N}^{f*})$ of system (3.1), so the numbers of residents in each patch and travelers from one patch to another are determined. More precisely,

$$\begin{aligned} N_j^* &= N_j^{u*} + N_j^{f*}, \quad 1 \le j \le p, \\ d_S c_{ij} N_j^* &= d_S c_{ij}^u N_j^{u*} + d_S c_{ij}^f N_j^{f*}, \quad 1 \le i, j \le p, \end{aligned}$$

where $\boldsymbol{N}^* = (N_1^*, \dots, N_p^*)$ is the unique equilibrium of system

$$\frac{dN_i}{dt} = \varepsilon_i - \mu_i N_i + d_S \sum_{j=1}^{p} c_{ij} N_j, \quad 1 \le i \le p.$$

Hence the movement rate from patch j to patch i is determined, i.e.,

$$c_{ij} = \frac{c_{ij}^u N_j^{u*} + c_{ij}^f N_j^{f*}}{N_j^{u*} + N_j^{f*}}. \tag{3.6}$$

In particular, if $c_{ij}^u \le c_{ij}^f$, then

$$c_{ij}^u \le c_{ij} \le c_{ij}^f,$$

that is, the movement rate of the traditional model lies between the movement rates of unfrequent and frequent travelers.

Clearly, the two models have the same recruitment rate ε_i. The natural death rate, transmission rate, and recovery rate in patch i of model (2.2) are, respectively, given by

$$\begin{aligned} \mu_i &= \frac{\mu_i^u N_j^{u*} + \mu_i^f N_j^{f*}}{N_i^{u*} + N_i^{f*}} = \frac{\varepsilon_i + d_S \sum_{j=1}^{p} (c_{ij}^u N_j^{u*} + c_{ij}^f N_j^{f*})}{N_i^{u*} + N_i^{f*}}, \\ \beta_i &= \frac{\beta_i^{uu} (N_i^{u*})^2 + \beta_i^{uf} N_i^{u*} N_i^{f*} + \beta_i^{fu} N_i^{f*} N_i^{u*} + \beta_i^{ff} (N_i^{f*})^2}{(N_i^*)^2}, \\ \gamma_i &= \frac{N_i^*}{N_i^{u*}/\gamma_i^u + N_i^{f*}/\gamma_i^f}. \end{aligned}$$

Remark 3.8. An alternative and possibly more reasonable way to derive the parameters β_i and γ_i of model (2.2) is to use the weights of both susceptible and infected populations instead of these of the total populations, namely,

$$\begin{aligned} \beta_i &= \frac{\beta_i^{uu} S_i^{u*} I_i^{u*} + \beta_i^{uf} S_i^{u*} I_i^{f*} + \beta_i^{fu} S_i^{f*} I_i^{u*} + \beta_i^{ff} S_i^{f*} I_i^{f*}}{S_i^* I_i^*}, \\ \gamma_i &= \frac{I_i^*}{I_i^{u*}/\gamma_i^u + I_i^{f*}/\gamma_i^f}, \end{aligned}$$

which agree with the above formulae if and only if $I_i^{u*}/N_i^{u*} = I_i^*/N_i^*$. In reality, the unfrequent travelers in the high transmission patch may suffer a higher risk of infection, leading to $I_i^{u*}/N_i^{u*} > I_i^*/N_i^*$. We will explore this point in the next section.

Recall that the basic reproduction number of model (2.2) is defined as $\bar{\mathcal{R}}_0 = \rho(\bar{F}\bar{V}^{-1})$, where $\bar{F} = \text{diag}\{\beta_1, \ldots, \beta_p\}$ and $\bar{V} = \text{diag}\{\gamma_1 + \mu_1, \ldots, \gamma_p + \mu_p\} - d_I C$. The model system (2.2) obeys the same threshold dynamics as the new model [18]. When two homogeneous patches, i.e., $\beta_i^{uu} = \beta_i^{uf} = \beta_i^{fu} = \beta_i^{ff}$, $\gamma_i^u = \gamma_i^f$, $\mu_i^u = \mu_i^f$ for $i = 1, 2$, without vital dynamics connected only by the movement of frequent travelers, are considered, the traditional model underestimates the risk of infection.

THEOREM 3.9. *Consider a two-patch submodel of* (2.3) *with* $\varepsilon_i = 0$, $\mu_i^u = \mu_i^f = 0$, $\beta_i^{uu} = \beta_i^{uf} = \beta_i^{fu} = \beta_i^{ff} = \beta_i$, $\gamma_i^u = \gamma_i^f = \gamma_i$ *for* $i = 1, 2$, *and* $c_{12}^u = c_{21}^u = 0$. *Then the reproduction number of the new model, denoted by* $\mathcal{R}_4$, *is always no less than that of the traditional model, denoted by* $\mathcal{R}_2$, *with equality if and only if* $\mathcal{R}_0^{(1)} = \mathcal{R}_0^{(2)}$, *or explicitly,* $\beta_1/\gamma_1 = \beta_2/\gamma_2$.

Proof. Under the above assumption, it follows from the first equation of (3.2) or Remark 3.5 or direct calculation of the disease-free equilibrium that

$$p_1 := \frac{N_1^{u*}}{N_1^*} = \frac{\phi_1^f}{\phi_1^u + \phi_1^f}, \quad \frac{N_1^{f*}}{N_1^*} = 1 - p_1, \quad p_2 := \frac{N_2^{u*}}{N_2^*} = \frac{\phi_2^f}{\phi_2^u + \phi_2^f}, \quad \frac{N_2^{f*}}{N_2^*} = 1 - p_2.$$

The incidence and transition matrices of the new model and traditional model are

$$F_4 = \begin{pmatrix} \beta_1 p_1 & 0 & \beta_1 p_1 & 0 \\ 0 & \beta_2 p_2 & 0 & \beta_2 p_2 \\ \beta_1(1-p_1) & 0 & \beta_1(1-p_1) & 0 \\ 0 & \beta_2(1-p_2) & 0 & \beta_2(1-p_2) \end{pmatrix},$$

$$V_4 = \begin{pmatrix} \gamma_1 + \phi_1^u & 0 & -\phi_1^f & 0 \\ 0 & \gamma_2 + \phi_2^u & 0 & -\phi_2^f \\ -\phi_1^u & 0 & \gamma_1 + \phi_1^f + d_I c_{21}^f & -d_I c_{12}^f \\ 0 & -\phi_2^u & -d_I c_{21}^f & \gamma_2 + \phi_2^f + d_I c_{12}^f \end{pmatrix},$$

and

$$F_2 = \begin{pmatrix} \beta_1 & 0 \\ 0 & \beta_2 \end{pmatrix} \quad \text{and} \quad V_2 = \begin{pmatrix} \gamma_1 + (1-p_1) d_I c_{21}^f & -(1-p_2) d_I c_{12}^f \\ -(1-p_1) d_I c_{21}^f & \gamma_2 + (1-p_2) d_I c_{12}^f \end{pmatrix},$$

respectively. Under a permutation transformation, F_4 is similar to

$$\bar{F}_4 = \begin{pmatrix} \beta_1 p_1 & \beta_1 p_1 & 0 & 0 \\ \beta_1(1-p_1) & \beta_1(1-p_1) & 0 & 0 \\ 0 & 0 & \beta_2 p_2 & \beta_2 p_2 \\ 0 & 0 & \beta_2(1-p_2) & \beta_2(1-p_2) \end{pmatrix}.$$

Note that $\text{rank}(F_4 V_4^{-1}) = \text{rank}(F_4) = \text{rank}(\bar{F}_4) = 2$. The characteristic equations of the next generation matrices $F_4 V_4^{-1}$ and $F_2 V_2^{-1}$ are, respectively,

$$(a_4\lambda^2 - b_4\lambda + c_4)\lambda^2 = 0 \quad \text{and} \quad a_2\lambda^2 - b_2\lambda + c_2 = 0,$$

where

$$\begin{aligned}
a_4 =& d_I c_{12}^f \gamma_1(\gamma_1+\phi_1^f+\phi_1^u)(\gamma_2+\phi_2^u)\\
&+\gamma_2(d_I c_{21}^f(\gamma_1+\phi_1^u)+\gamma_1(\gamma_1+\phi_1^f+\phi_1^u))(\gamma_2+\phi_2^f+\phi_2^u),\\
b_4 =& ((\beta_1\gamma_2+\beta_2\gamma_1)(\gamma_1+\phi_1^f+\phi_1^u)+d_I c_{21}^f(p_1\beta_1\gamma_2+\beta_2(\gamma_1+\phi_1^u)))(\gamma_2+\phi_2^f+\phi_2^u)\\
&+d_I c_{12}^f(\gamma_1+\phi_1^f+\phi_1^u)(p_2\beta_2\gamma_1+\beta_1(\gamma_2+\phi_2^u)),\\
c_4 =& \beta_1\beta_2(p_2 d_I c_{12}^f(\gamma_1+\phi_1^f+\phi_1^u)+(p_1 d_I c_{21}^f+\gamma_1+\phi_1^f+\phi_1^u)(\gamma_2+\phi_2^f+\phi_2^u))
\end{aligned}$$

and

$$\begin{aligned}
a_2 &= (1-p_2)d_I c_{12}^f\gamma_1+(1-p_1)d_I c_{21}^f\gamma_2+\gamma_1\gamma_2,\\
b_2 &= (1-p_2)d_I c_{12}^f\beta_1+(1-p_1)d_I c_{21}^f\beta_2+\beta_1\gamma_2+\beta_2\gamma_1,\\
c_2 &= \beta_1\beta_2
\end{aligned}$$

are positive. Thus, the basic reproduction numbers of the new model and the traditional model are, respectively,

$$\mathcal{R}_4=\frac{b_4+\sqrt{b_4^2-4a_4c_4}}{2a_4} \quad \text{and} \quad \mathcal{R}_2=\frac{b_2+\sqrt{b_2^2-4a_2c_2}}{2a_2}.$$

Direct calculation yields

$$a_2b_4-a_4b_2=\frac{c_{12}^f\beta_2\gamma_1^2(\phi_1^f+\phi_1^u)\phi_2^u+c_{21}^f\beta_1\gamma_2^2(\phi_2^f+\phi_2^u)\phi_1^u}{(\phi_1^f+\phi_1^u)^2(\phi_2^f+\phi_2^u)^2}\rho>0$$

and

$$(a_2b_4-a_4b_2)(b_2c_4-b_4c_2)-(a_2c_4-a_4c_2)^2=\frac{c_{12}^f c_{21}^f\beta_1\beta_2\phi_1^u\phi_2^u(\beta_1\gamma_2-\beta_2\gamma_1)^2}{(\phi_1^f+\phi_1^u)^3(\phi_2^f+\phi_2^u)^3}\rho^2\geq 0$$

with $\rho=d_I^2c_{12}^f\phi_2^f(\phi_1^f+\phi_1^u)(\gamma_1+\phi_1^f+\phi_1^u)+d_I^2c_{21}^f\phi_1^f(\phi_2^f+\phi_2^u)(\gamma_2+\phi_2^f+\phi_2^u)$. Therefore,

$$\begin{aligned}
&(a_2b_4-a_4b_2)(b_2c_4-b_4c_2)\geq(a_2c_4-a_4c_2)^2\\
\Leftrightarrow&(b_2^2-4a_2c_2)(b_4^2-4a_4c_4)\geq(b_2b_4-2a_4c_2-2a_2c_4)^2\\
\Rightarrow&\sqrt{b_2^2-4a_2c_2}\sqrt{b_4^2-4a_4c_4}\geq b_2b_4-2a_4c_2-2a_2c_4\\
\Leftrightarrow&(a_2b_4-a_4b_2)^2\geq\left(a_4\sqrt{b_2^2-4a_2c_2}-a_2\sqrt{b_4^2-4a_4c_4}\right)^2\\
\Rightarrow&a_2b_4-a_4b_2\geq a_4\sqrt{b_2^2-4a_2c_2}-a_2\sqrt{b_4^2-4a_4c_4},
\end{aligned}$$

the last inequality being equivalent to $\mathcal{R}_4\geq R_2$. ∎

The above result fails to hold in a heterogeneous setting, but extensive numerical calculations suggest that it mostly remains true when parameter values are reasonably chosen. Biologically, these mean that the traditional model underestimates the risk of infection and the new model has some advantages in describing the spread of infectious diseases in discrete space. In other words, the new model differs from the traditional model even if there is no epidemiological or demographical difference between unfrequent and frequent travelers within the patch.

Remark 3.10. The inequality $\min_{1\le i\le p}\mathcal{R}_0^{(i)} \le \mathcal{R}_0 \le \max_{1\le i\le p}\mathcal{R}_0^{(i)}$ generally fails for the new model (2.3) even if $d_S = d_I$, which is different from the traditional model [18]. Thus heterogeneity in travel frequency is a mechanism to intensify or weaken the disease persistence among patches.

We will numerically compare the traditional model and the new model through the risk of infection and disease prevalence in the next section.

4. Numerical simulations. In the two-patch case, we numerically investigate the importance of addressing travel differences and the influence of changes in global travel on the geographic spread of infectious diseases. Due to economic development and technological progress, human travel and tourism are experiencing unprecedented changes in both global and regional scales:

(1) more people move from unfrequent traveler group to frequent traveler group, i.e., increase ϕ_i^u or decrease ϕ_i^f, which leads to a higher proportion of frequent travelers within patch i as a result of Proposition 3.6;
(2) travelers move more frequently than ever before, which can be achieved by increasing the diffusion coefficients d_S and d_I;
(3) travelers move more rapidly, which means the duration of travel from one patch to another is sharply shortened.

We focus on the first two changes but skip the last one since our model does not consider the infection during transport [9, 30]. The parameter ranges in Table 1 are primarily based on the transmission and epidemiology of the common cold with per day as the default time unit [35, 37, 41, 42].

TABLE 1
The parameters for the model (2.3) *and their ranges.*

	Description	Range
ε_i	recruitment rate	1–10
θ_i	proportion of recruited susceptibles being frequent travelers	0–0.5
β_i^{kl}	transmission rate between S_i^k and I_i^l with $k,l = u$ or f	0.05–0.3
γ_i^k	recovery rate of infectious unfrequent and infectious frequent travelers with $k = u$ and f, respectively	0.05–0.15
μ_i^k	mortality rate of unfrequent and frequent travelers with $k = u$ and f, respectively	3.2×10^{-5} –5.5×10^{-5}
ϕ_i^f	exchange rate from frequent group to unfrequent group	2.7×10^{-4} –9×10^{-4}
τ_i	relative transfer rate of unfrequent group to frequent group	0.1-0.5
ϕ_i^u	exchange rate from unfrequent group to frequent group	$\phi_i^u = \tau_i\phi_i^f$
c_{ij}^f	movement rate of frequent group from patch j to patch i	0.03–0.1
τ_{ij}	relative travel rate of unfrequent group to frequent group	0–0.4
c_{ij}^u	movement rate of unfrequent group from patch j to patch i	$c_{ij}^u = \tau_{ij}c_{ij}^f$
d_S	diffusion coefficient of the susceptible subpopulation	1
d_I	diffusion coefficient of the infected subpopulation	0–1

Example 4.1 (underestimate or overestimate the risk of infection). Consider the new model (2.3) with the parameter setting $\varepsilon_1 = 5, \varepsilon_2 = 2, \theta_1 = 0.3, \theta_2 = 0.1$, $\beta_1^{uu} = \beta_1^{uf} = \beta_1^{fu} = \beta_1^{ff} = 0.07$, $\beta_2^{uu} = \beta_2^{uf} = \beta_2^{fu} = \beta_2^{ff} = 0.143$, $\gamma_1^u = \gamma_1^f = \gamma_2^u = \gamma_2^f = 0.12$, $\mu_1^u = \mu_1^f = 3.5\times10^{-5}$, $\mu_2^u = \mu_2^f = 4\times10^{-5}$, $\phi_1^u = 1.2\times10^{-4}, \phi_1^f = 5\times10^{-4}$, $\phi_2^u = 1.5\times10^{-4}, \phi_2^f = 5\times10^{-4}, d_S = d_I = 1$. The parameter values of the corresponding traditional model are $\beta_1 = 0.07, \beta_2 = 0.143, \mu_1 = 3.5\times10^{-5}, \mu_2 = 4\times10^{-5}, \gamma_1 = \gamma_2 = 0.12$. The respective basic reproduction numbers of the disease

in patches 1 and 2 are $\mathcal{R}_0^{(1)} = 0.5832$ and $\mathcal{R}_0^{(2)} = 1.1913$. Thus, the disease goes extinct in patch 1 but persists in patch 2. When the two patches are connected by human movement with $c_{12}^f = 0.08, c_{21}^f = 0.04$ and $c_{12}^u = \tau_{12}c_{12}^f, c_{21}^u = \tau_{21}c_{21}^f$ for $\tau_{12}, \tau_{21} \in [0, 1]$, the difference between the reproduction numbers of the new model and the traditional model, $\mathcal{R}_0 - \bar{\mathcal{R}}_0$, versus τ_{12} and τ_{21} is plotted in Figure 2. For example, if $\tau_{12} = \tau_{21} = 0.25$, then $c_{12}^u = 0.02$ and $c_{21}^u = 0.01$ so that $\mathcal{R}_0 = 1.0052$, that is, human movement promotes the disease spread in low transmission regions. Meanwhile, direct computation gives

$$(N_1^{u*}, N_2^{u*}, N_1^{f*}, N_2^{f*}) \approx (100796, 50341, 26513, 13264)$$

and hence it follows from (3.6) that $c_{12} = 0.0325$ and $c_{21} = 0.0162$. So the reproduction number of the traditional model is $\bar{\mathcal{R}}_0 = 0.9897$. In the current parameter setting, $\mathcal{R}_0$ is no less than $\bar{\mathcal{R}}_0$ with equality if and only if $\tau_{12} = \tau_{21} = 1$ (under which the new model can be reduced to the traditional model). This suggests that ignoring travel differences leads to underestimation of the risk of infection.

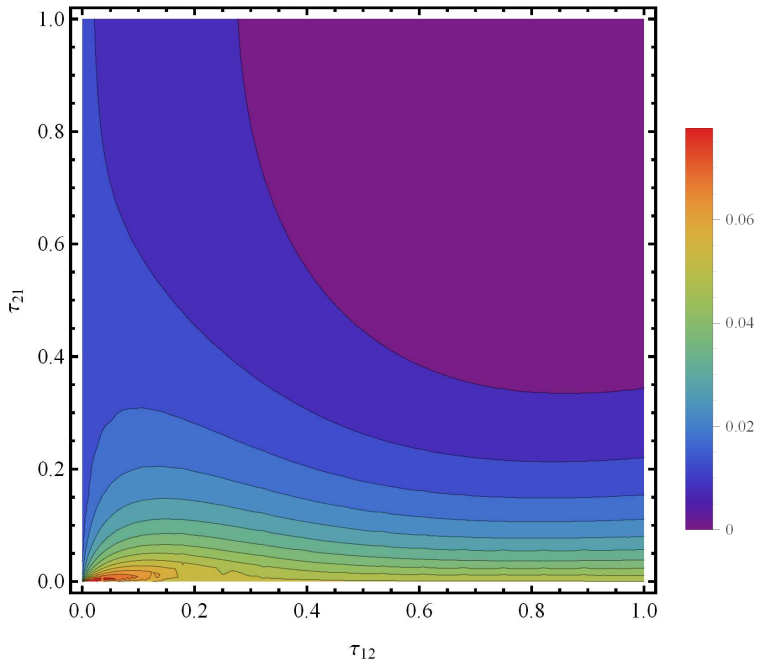

FIG. 2. *The contour plot of the difference of the reproduction numbers of the new model and that of the corresponding traditional model, $\mathcal{R}_0 - \bar{\mathcal{R}}_0$, with respect to relative travel rates τ_{12} and τ_{21}.*

Moreover, under the homogeneous assumption and the biologically reasonable restriction $\phi_i^u = \tau_i \phi_i^f$ and $c_{ij}^u = \tau_{ij} c_{ij}^f$ for $i, j = 1, 2$ and $i \neq j$, we use the Latin hypercube sampling (LHS) method to randomly generate 10^5 parameter sets with the parameter ranges in Table 1. We find 238 scenarios where the traditional model overestimates the infection risk with the maximum difference less than 3.6×10^{-5}. Surprisingly, under a weakly homogeneous assumption, i.e., the assumption $\beta_i^{uu} = \beta_i^{uf} = \beta_i^{fu} = \beta_i^{ff}$ is weakened to $\beta_i^{uf} = \beta_i^{fu}$, only nine scenarios have $\mathcal{R}_0$ less than $\bar{\mathcal{R}}_0$, with the maximum difference being around 4.2×10^{-5}. Even if we set

$\tau_i \in [0,1]$ and $\tau_{ij} \in [0,1]$, there are only 734 scenarios where $\bar{\mathcal{R}}_0 - \mathcal{R}_0$ is positive with the maximum difference less than 1.1×10^{-4}. Therefore, the traditional model tends to underestimate the disease transmission risk. However, when the assumption $\beta_i^{uu} = \beta_i^{uf} = \beta_i^{fu} = \beta_i^{ff}$ is removed, 26,922 scenarios are obtained with the maximum difference being about 0.36.

In addition, under the homogeneous assumption, it follows from Proposition 2.2 in Gao and Ruan [18] and Theorem 3.1 that $\mathcal{R}_0$ and $\bar{\mathcal{R}}_0$ satisfy

$$\min_{1\le i\le p} \mathcal{R}_0^{(i)} \le \mathcal{R}_0 \le \max_{1\le i\le p} \mathcal{R}_0^{(i)} \quad \text{and} \quad \min_{1\le i\le p} \mathcal{R}_0^{(i)} \le \bar{\mathcal{R}}_0 \le \max_{1\le i\le p} \mathcal{R}_0^{(i)},$$

where $\mathcal{R}_0^{(i)} = \mathcal{R}_i^{uu} = \mathcal{R}_i^{uf} = \mathcal{R}_i^{fu} = \mathcal{R}_i^{ff}$. Nevertheless, the inequality for $\mathcal{R}_0$ does not hold when the homogeneous assumption fails. For example, using the same parameter setting for model (2.3) as the above specific example except that $c_{12}^u = 0.02, c_{21}^u = 0.01$ and the transmission rates, if $\beta_1^{uu} = 0.116, \beta_1^{uf} = \beta_1^{fu} = 0.26, \beta_1^{ff} = 0.235$, $\beta_2^{uu} = 0.158, \beta_2^{uf} = \beta_2^{fu} = 0.213$, and $\beta_2^{ff} = 0.133$, then $\mathcal{R}_0 = 1.4735 > \max\{\mathcal{R}_0^{(1)}, \mathcal{R}_0^{(2)}\} = \{1.4678, 1.4692\}$; if $\beta_1^{uu} = 0.23, \beta_1^{uf} = \beta_1^{fu} = 0.078, \beta_1^{ff} = 0.078$, $\beta_2^{uu} = 0.13, \beta_2^{uf} = \beta_2^{fu} = 0.25$, and $\beta_2^{ff} = 0.27$, then $\mathcal{R}_0 = 1.5286 < \min\{\mathcal{R}_0^{(1)}, \mathcal{R}_0^{(2)}\} = \{1.5802, 1.5549\}$.

Example 4.2 (more frequent travelers). By choosing four parameter sets (see the supplement material SM1) with ranges in Table 1 and under the homogeneous assumption, we show their corresponding contour plots of $\mathcal{R}_0$ versus the relative frequency exchange rates τ_1 and τ_2 in Figure 3. Note that an increase in τ_i, or equivalently ϕ_i^u, gives a higher fraction of frequent travelers of patch i provided that all other parameters are fixed. In Figure 3a, increasing the exchange rate from unfrequent group to frequent group in either patch produces a larger $\mathcal{R}_0$. Figure 3b illustrates a scenario in which $\mathcal{R}_0$ is reduced by increasing any of τ_1 and τ_2. Figure 3c is the scenario where a larger $\mathcal{R}_0$ is generated through decreasing τ_1 or increasing τ_2. The last subfigure depicts the nonmonotonic dependence of $\mathcal{R}_0$ in τ_1 and τ_2. These suggest that the influence of changes in the exchange rate and hence the fraction of frequent travelers on the disease persistence can only be determined via a case-by-case study.

Example 4.3 (higher travel frequency). We examine the dependence of the reproduction number $\mathcal{R}_0$ on the diffusion coefficient of the infected subpopulation d_I. Under the homogeneous assumption and within parameter ranges in Table 1, we again use the LHS method to generate 10^5 random parameter sets among which 99,796 scenarios have $\mathcal{R}_0$ decreasing in d_I (see Figure 4a) and 204 scenarios have $\mathcal{R}_0$ initially decreasing and then increasing in d_I (see Figure 4b). The reason that no scenario has $\mathcal{R}_0$ initially increasing in d_I is that under the homogeneous assumption we have $\min\{\mathcal{R}_1^{uu}, \mathcal{R}_2^{uu}\} \le \mathcal{R}_0(d_I) \le \max\{\mathcal{R}_1^{uu}, \mathcal{R}_2^{uu}\} = \mathcal{R}_0(0)$ by Theorem 3.1 and Corollary 3.3. However, under weakly homogeneous assumption, the numbers of decreasing, increasing, and nonmonotonic scenarios become 43,906, 4, and 56,090, respectively. An increasing scenario is plotted in Figure 4c, while three additional nonmonotonic scenarios besides the one in Figure 4b are plotted in Figures 4d–4f. Moreover, over 90% (50,885) of nonmonotonic scenarios have $\mathcal{R}_0(0)$ greater than $\mathcal{R}_0(100)$. Thus sufficiently fast diffusion mostly alleviates the persistence of disease.

Allen et al. [1] conjectured that the basic reproduction number $\bar{\mathcal{R}}_0$ of the traditional model (2.2) is a monotone decreasing function of the diffusion coefficient for the infected subpopulation d_I if the connectivity matrix C is quasi-positive, irreducible, and symmetric. In the appendix, we confirm the conjecture for an environment with an arbitrary number of patches. Furthermore, the conjecture is still true even for

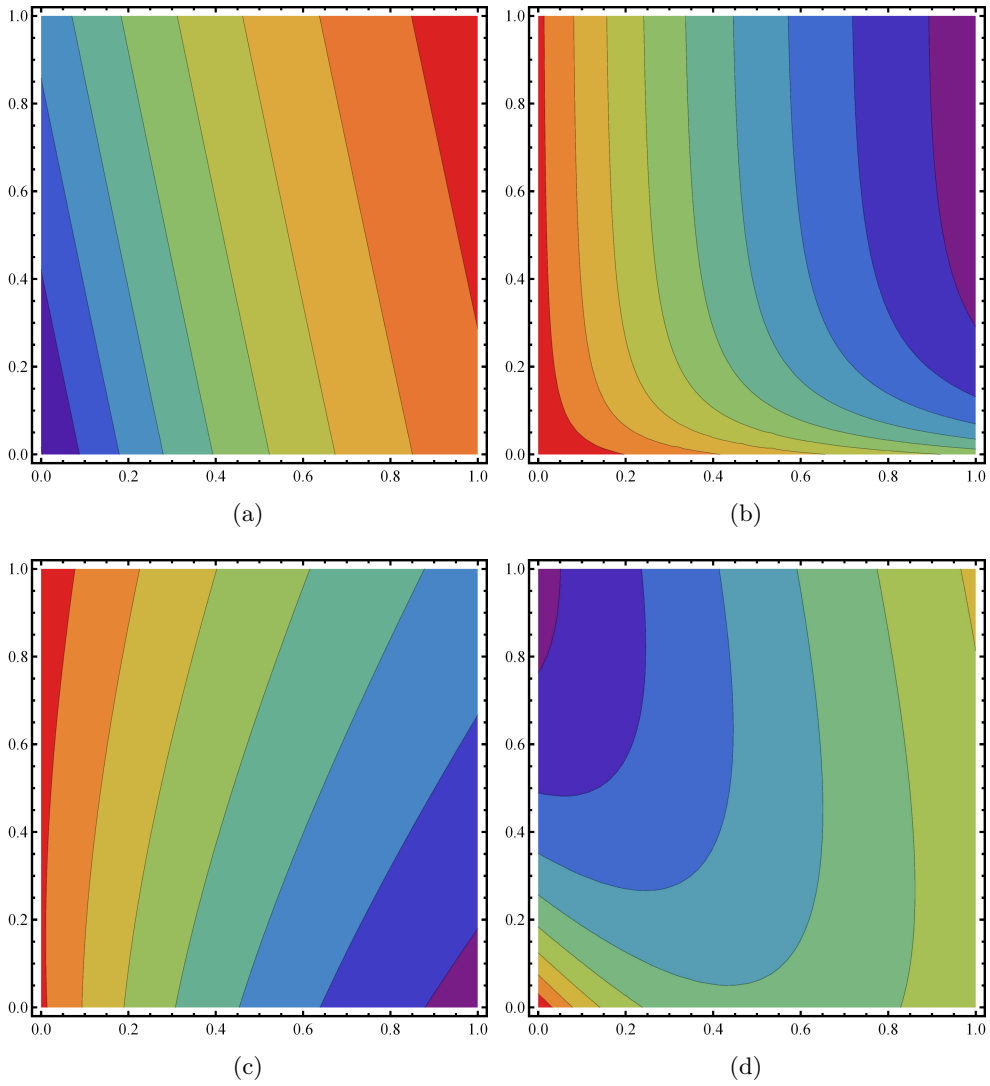

FIG. 3. *The contour plot of the reproduction number $\mathcal{R}_0$ under four different scenarios. The x- and y- axes represent the relative frequency exchange rates τ_1 and τ_2, respectively. The color scheme is the same as that of Figure* 2 *with color varying from purple to red. (Figure in color online.)*

the model (2.2) with asymmetric connectivity matrix [16]. Particularly, the two-patch case can be rigorously proved by direct algebraic manipulation. In contrast, the above analysis finds that the decreasing monotonicity fails for the new model (2.3) even under the homogeneous assumption, and the nonmonotonic dependence is very common under the weakly homogeneous assumption. This difference again emphasizes the importance of distinguishing travel frequency in spatial epidemic models.

Example 4.4 (implication for disease control). With limited health resources, an allocation strategy that can minimize the disease burden is preferred. People who have a higher risk of getting infections may require more preventive care. In our model the question is: which is the high risk group, the unfrequent travelers N_i^u or

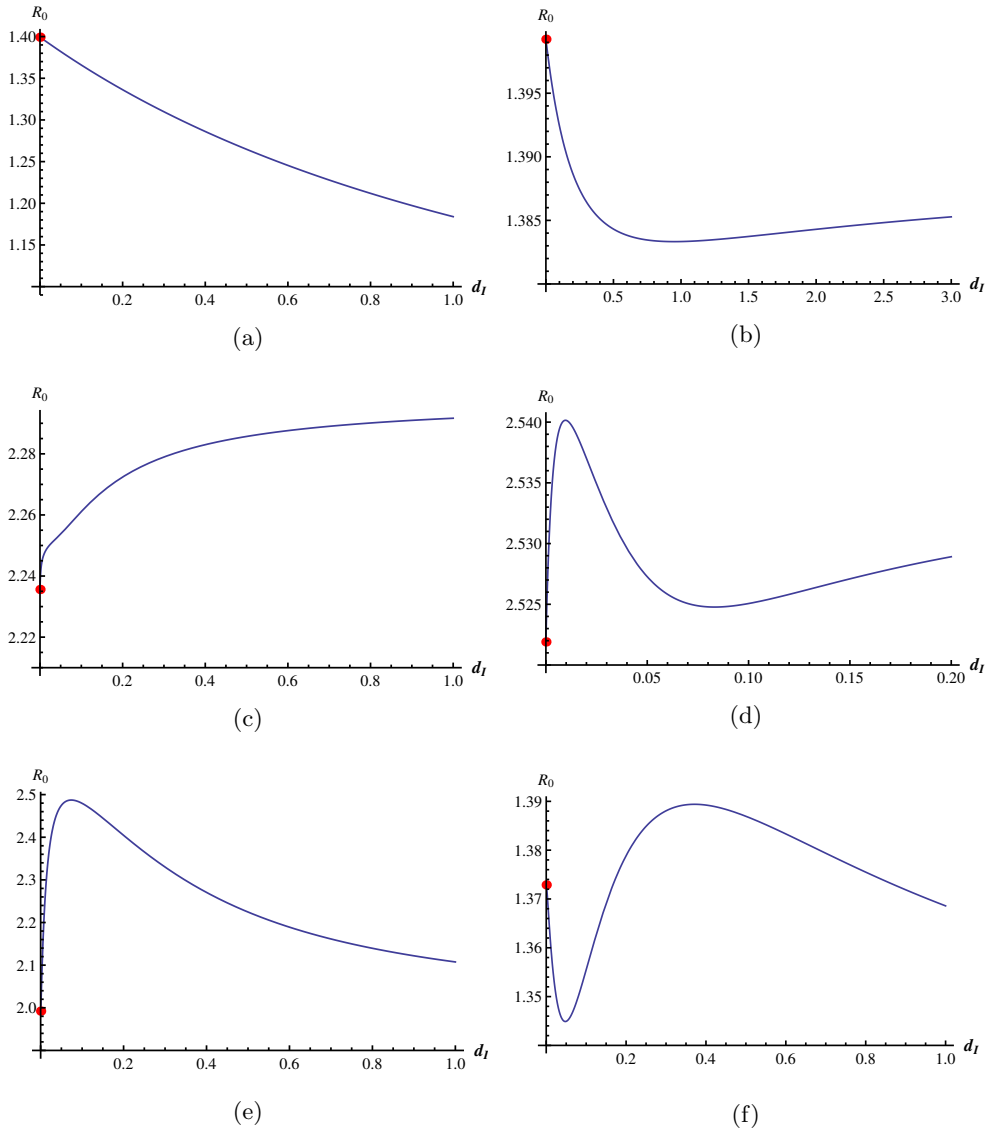

FIG. 4. *Relationship between the reproduction number $\mathcal{R}_0$ and the diffusion coefficient d_I under six different scenarios. The first two scenarios are under homogeneous assumption while the remaining are under weakly homogeneous assumption. See* SM2 *for parameter values of each scenario.*

frequent travelers N_i^f? Mathematically, we need to compare the disease prevalences of the unfrequent and frequent groups within each patch or across both patches at the endemic equilibrium,

$$\frac{I_i^{u*}}{N_i^{u*}} : \frac{I_i^{f*}}{N_i^{f*}} \quad \text{for} \quad i = 1, 2 \quad \text{or} \quad \frac{\sum_{i=1}^2 I_i^{u*}}{\sum_{i=1}^2 N_i^{u*}} : \frac{\sum_{i=1}^2 I_i^{f*}}{\sum_{i=1}^2 N_i^{f*}},$$

respectively. For the simplicity of solving the endemic equilibrium, we assume that $d_S = d_I = 1$, which also agrees with the fact that the common cold is mostly not

severe enough to impair mobility. However, similar conclusions can be drawn for the case of $d_I < d_S$. Under the homogeneous assumption and within the parameter ranges in Table 1, we randomly generate 10^5 parameter sets and obtain 94,080 scenarios whose reproduction numbers are greater than one. Among these qualified scenarios, after performing the first comparison, 185 have frequent travelers of both patches being high risk groups (maximum absolute difference in disease prevalence less than 0.03), 54 have unfrequent travelers of both patches being high risk groups (maximum absolute difference in disease prevalence near 0.0004), and the remaining 93,841 have unfrequent travelers of one patch and frequent travelers of the other patch being high risk groups. More specifically, 93,818 of the 93,841 scenarios have unfrequent travelers in the high transmission patch (where the patch reproduction number is bigger) and frequent travelers in the low transmission patch (where the patch reproduction number is smaller) being high risk groups. When the disease prevalences of all four subpopulations are compared, the number of scenarios representing unfrequent travelers in the high transmission patch being the highest risk group and unfrequent travelers in the low transmission patch being the lowest risk group are, respectively, 93,865 and 93,975. Therefore, in the case of two homogeneous patches, the high risk group within a patch almost completely comes from unfrequent travelers in high transmission regions and frequent travelers in low transmission regions; the highest and lowest risk groups almost completely come from unfrequent travelers in high and low transmission patches, respectively. It is understandable that leaving high transmission regions or staying in low transmission regions are helpful in reducing infection risk. A comparison of the average disease prevalences of unfrequent and frequent travelers across two patches finds the number of scenarios representing unfrequent and frequent traveler groups being at higher risk of infection are, respectively, 49,398 and 44,682. However, with the first comparison, both the percentage of scenarios that frequent or unfrequent travelers of both patches are high risk groups and the maximum absolute difference in disease prevalence increase sharply under weakly homogeneous assumption or within enlarged parameter ranges.

Without loss of generality, we now consider a two-patch environment where the transmission risk of patch 1 is higher than that of patch 2, i.e., $\mathcal{R}_0^{(1)} > \mathcal{R}_0^{(2)}$. Health campaigns reduce transmission rates β_1^{uu} and β_1^{uf} for unfrequent travelers in high transmission regions, N_1^{u*}, β_1^{fu} and β_1^{ff} for frequent travelers in high transmission regions, N_1^{f*}, β_2^{uu} and β_2^{uf} for unfrequent travelers in low transmission regions, N_2^{u*}, β_2^{fu} and β_2^{ff} for frequent travelers in low transmission regions, N_2^{f*}, respectively. Given a fixed amount of health resources, we ask: which exclusive allocation approach can produce the largest reduction in the number of infections or the reproduction number? Suppose that the reduction in the amplitude of transmission rate is proportional to the per capita resource availability regardless of travel frequency and residence. The same amount of resources can be used to, respectively, reduce the transmission rates

$$\begin{aligned}
&\beta_1^{uu} \text{ and } \beta_1^{uf} \text{ for } N_1^{u*} \text{ to } (1-\delta m/N_1^{u*})\beta_1^{uu} \text{ and } (1-\delta m/N_1^{u*})\beta_1^{uf},\\
&\beta_1^{fu} \text{ and } \beta_1^{ff} \text{ for } N_1^{f*} \text{ to } (1-\delta m/N_1^{f*})\beta_1^{fu} \text{ and } (1-\delta m/N_1^{f*})\beta_1^{ff},\\
&\beta_2^{uu} \text{ and } \beta_2^{uf} \text{ for } N_2^{u*} \text{ to } (1-\delta m/N_2^{u*})\beta_2^{uu} \text{ and } (1-\delta m/N_2^{u*})\beta_2^{uf},\\
&\beta_2^{fu} \text{ and } \beta_2^{ff} \text{ for } N_2^{f*} \text{ to } (1-\delta m/N_2^{f*})\beta_2^{fu} \text{ and } (1-\delta m/N_2^{f*})\beta_2^{ff},
\end{aligned}$$

where $\delta \in [0,1]$ represents the reduced fraction of the transmission rate due to medical resources and $m = \min\{N_1^{u*}, N_1^{f*}, N_2^{u*}, N_2^{f*}\}$. Under homogeneous assumption and within the parameter ranges in Table 1, we generate 10^4 random parameter sets

leading to 8,710 scenarios whose reproduction numbers after resource allocation remain greater than one. Among these 8,710 scenarios, the number of scenarios wherein allocation to $N_1^{u*}, N_1^{f*}, N_2^{u*}$, and N_2^{f*} constantly yields the largest reduction in infections are, respectively, 166, 4,924, 197, and 416, and the second largest reductions are, respectively, 3,856, 209, 369, and 145 (see Figure 5a). The number of scenarios that allocation to $N_1^{u*}, N_1^{f*}, N_2^{u*}$, and N_2^{f*} constantly yields the largest reduction in the reproduction number are, respectively, 6,787, 1, 0, and 196, and the second largest reduction are, respectively, 1, 6,784, 168, and 0 (see Figure 5b). As $\delta \to 1$, the number of scenarios wherein allocation to N_1^{f*} yields the largest reduction in infections and to N_1^{u*} yields the largest reduction in reproduction number are, respectively, 6,618 and 6,902. So allocating resources towards frequent travelers in high transmission regions and unfrequent travelers in high transmissions region are possibly the most effective strategies in reducing infections and the reproduction number, respectively. Nevertheless, targeting interventions to frequent travelers in low transmission regions may work better in a few scenarios. Figures 5c–5d show that the optimal allocation strategy in terms of infection size and reproduction number may vary with the per capita resources availability.

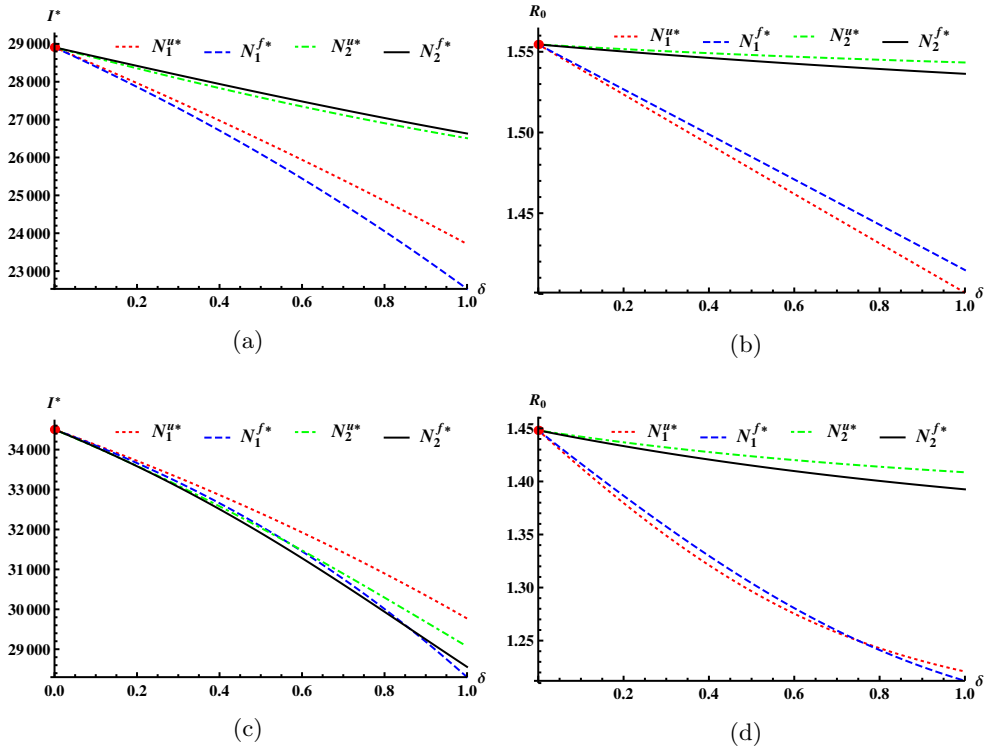

FIG. 5. *Total number of infections and the reproduction number versus the reduced fraction of transmission rate under four allocation strategies. See* SM3 *for parameter values of each scenario.*

5. Discussion. In this paper, we proposed an epidemic patch model aimed at capturing the fact that travel frequency varies widely from person to person. The dynamics of each patch in isolation are described by a simple two-group SIS model, incorporating unfrequent and frequent travelers. We derive the basic reproduction

number $\mathcal{R}_0$ that completely determines the global dynamics of the model if the diffusion coefficients for susceptible and infective individuals are the same. Namely, the disease-free equilibrium is globally asymptomatically stable if $\mathcal{R}_0 \leq 1$, and the model admits a unique endemic equilibrium which is globally asymptomatically stable if $\mathcal{R}_0 > 1$. Mathematically tractable and biologically meaningful bounds on $\mathcal{R}_0$ are established. We compared our model with the model that ignores the difference in travel frequency through both analytical and numerical approaches and showed that the latter usually underestimates the risk of infection when a homogeneous or weakly homogeneous assumption and biologically reasonable parameter ranges are taken.

Three additional numerical examples were given to illustrate the impact of changes in modern transportation on disease spread and control [39]. The first example focused on the trend that more people are traveling frequently. We studied the dependence of the reproduction number $\mathcal{R}_0$ on the relative frequency exchange rates τ_1 and τ_2 of patches 1 and 2, respectively, and found that $\mathcal{R}_0$ could be simultaneously increasing or decreasing, or inconsistently monotone, or nonmonotonic with respect to τ_1 and τ_2. Thus, changes in the proportion of frequent travelers may affect the infection risk in a complicated way. The second example treated the change that people are traveling more often than ever before. Under the homogeneous assumption and proper parameter ranges, we found that increasing the diffusion coefficient, d_I, almost always reduces $\mathcal{R}_0$ but occasionally first decreases then increases $\mathcal{R}_0$. Moreover, under the weakly homogeneous assumption, the possibility of nondecreasing dependence is even higher than that of decreasing dependence, and strictly increasing dependence could happen. Furthermore, the nondecreasing dependence has at least five patterns (see Figure 4b–4f). However, sufficiently fast diffusion mostly weakens the disease spread. The last example considered the implication of the current study to disease control in an environment with two homogeneous patches. On the one hand, the high risk groups in high and low transmission regions are, respectively, the unfrequent and frequent travelers, and individuals who travel less frequently in the high transmission region suffer the highest risk of infection. On the other hand, possibly the best resource management to reduce infections and the reproduction number is to distribute resources to frequent and unfrequent travelers in high transmission regions, respectively. With regard to application, the subdivision of population in the new model makes the recognition of individuals at high infection risk much easier and resource management for disease control more efficient.

The study presented here is only a first step toward understanding the influence of heterogeneity in travel frequency on the spatial and temporal spread of infectious diseases. There are various directions to improve and generalize. The dependence of the multipatch basic reproduction number $\mathcal{R}_0$ with respect to model parameters such as the frequency exchange rate and the diffusion coefficient deserve detailed study. Like the work of Allen et al. [1], it is necessary to analyze the asymptotic profiles of the endemic equilibrium with respect to diffusion coefficients which have important implications for disease control. We assumed a homogeneous mixing of the population in each patch. However, in reality, frequent travelers often make more contacts with each other than people outside their group and hence a heterogeneous mixing population is more realistic [21, 23]. The model can be generalized to consist of a finite number or even a continuum of travel frequencies, e.g., low, medium, and high frequency. Some infectious diseases are fatal, or disproportionately impair the mobility of infectives, or have complicated life cycles (induce more disease states), or involve a vector population, or transmit via multiple routes. The difference in the frequency and destination of local commutes also exists, that is, some people commute

every business day while others stay home or nearby. This can be modeled by using the so-called Lagrangian approach, in which movement to another patch does not change the residence of an individual [8, 12, 22]. A change of residence has a high potential to adjust a person's travel behavior, e.g., moving closer to the workplace. To assess the validity of the model, we particularly need to conduct a systematic survey on travel behavior and contact pattern to estimate the matrices for movement rates, frequency exchange rates, and transmission rates.

Appendix A. Proof of the conjecture for model (2.2).

THEOREM A.1. *Let $F = \operatorname{diag}\{\beta_1, \dots, \beta_p\}$ and $D = \operatorname{diag}\{\gamma_1, \dots, \gamma_p\}$ be two positive diagonal matrices, and let $L = (L_{ij})_{p\times p}$ be a quasi-positive, irreducible, and symmetric matrix with zero column sums. Then $\mathcal{R}_0 := \rho(FV^{-1})$ with $V = D - \tau L$ is either constant or strictly decreasing in $\tau \in [0, \infty)$ and $\mathcal{R}_0'(\tau) < 0$ for $\tau \in (0, \infty)$.*

Proof. If $F = mD$ for some $m > 0$, then it is easy to see that $\mathcal{R}_0 = m$ is constant. So it suffices to consider the case where F is not a scalar multiple of D.

By the Perron–Frobenius theorem, there is a unique column vector $\boldsymbol{v} := \boldsymbol{v}(\tau) \gg 0$ with $\boldsymbol{v}^T\boldsymbol{v} = 1$ such that

$$V^{-1}F\boldsymbol{v} = \rho(V^{-1}F)\boldsymbol{v} = \rho(FV^{-1})\boldsymbol{v} = \mathcal{R}_0\boldsymbol{v},$$

which implies that $(F - \mathcal{R}_0 V)\boldsymbol{v} = 0$, or equivalently,

$$((kI_n + F - \mathcal{R}_0 D) + \tau\mathcal{R}_0 L)\boldsymbol{v} = k\boldsymbol{v} \quad \text{for } \ k \in \mathbb{R}.$$

Choosing sufficiently large k gives a symmetric matrix

$$A := A(\tau) = (kI_n + F - \mathcal{R}_0 D) + \tau\mathcal{R}_0 L$$

that is nonnegative and irreducible. Again by the Perron–Frobenius theorem, $\rho(A) = k$ is an algebraically simple eigenvalue for matrix A. Differentiating the equality

$$\boldsymbol{v}^T A\boldsymbol{v} = \rho(A)\boldsymbol{v}^T\boldsymbol{v} = k$$

with respect to τ yields

$$\begin{aligned}
0 = \frac{d(\boldsymbol{v}^T A\boldsymbol{v})}{d\tau} &= \frac{d\boldsymbol{v}^T}{d\tau}A\boldsymbol{v} + \boldsymbol{v}^T\frac{dA}{d\tau}\boldsymbol{v} + \boldsymbol{v}^T A\frac{d\boldsymbol{v}}{d\tau} = \frac{d\boldsymbol{v}^T}{d\tau}\rho(A)\boldsymbol{v} + \boldsymbol{v}^T\frac{dA}{d\tau}\boldsymbol{v} + \rho(A)\boldsymbol{v}^T\frac{d\boldsymbol{v}}{d\tau} \\
&= \rho(A)\left(\frac{d\boldsymbol{v}^T}{d\tau}\boldsymbol{v} + \boldsymbol{v}^T\frac{d\boldsymbol{v}}{d\tau}\right) + \boldsymbol{v}^T\frac{dA}{d\tau}\boldsymbol{v} = \rho(A)\frac{d(\boldsymbol{v}^T\boldsymbol{v})}{d\tau} + \boldsymbol{v}^T\frac{dA}{d\tau}\boldsymbol{v} = \boldsymbol{v}^T\frac{dA}{d\tau}\boldsymbol{v} \\
&= \boldsymbol{v}^T\left(-\frac{d\mathcal{R}_0}{d\tau}D + \frac{d\mathcal{R}_0}{d\tau}\tau L + \mathcal{R}_0 L\right)\boldsymbol{v} = \boldsymbol{v}^T\left(-\frac{d\mathcal{R}_0}{d\tau}V + \mathcal{R}_0 L\right)\boldsymbol{v} \\
&= \boldsymbol{v}^T\left(-\frac{d\mathcal{R}_0}{d\tau}\frac{1}{\mathcal{R}_0}F + \mathcal{R}_0 L\right)\boldsymbol{v} = -\frac{d\mathcal{R}_0}{d\tau}\frac{1}{\mathcal{R}_0}\boldsymbol{v}^T F\boldsymbol{v} + \mathcal{R}_0\boldsymbol{v}^T L\boldsymbol{v}.
\end{aligned}$$

Claim: $\boldsymbol{v}^T L\boldsymbol{v} < 0$. Since L is a quasi-positive, irreducible, symmetric matrix with zero column sums, by the Perron–Frobenius theorem, the spectrum of L is $\sigma(L) = \{0, \lambda_2, \dots, \lambda_p\}$ with $\lambda_i < 0$ for $i = 2, \dots, p$. Using the Gram–Schmidt process, there exists an orthogonal matrix

$$Q = \begin{pmatrix} q_{11} & q_{12} & \cdots & q_{1p} \\ q_{21} & q_{22} & \cdots & q_{2p} \\ \vdots & \vdots & \ddots & \vdots \\ q_{p1} & q_{p2} & \cdots & q_{pp} \end{pmatrix} = \begin{pmatrix} \boldsymbol{q}_1^T \\ \boldsymbol{q}_2^T \\ \vdots \\ \boldsymbol{q}_p^T \end{pmatrix}$$

such that

$$QLQ^T = \operatorname{diag}\{0, \lambda_2, \dots, \lambda_p\},$$

where $\boldsymbol{q}_1^T = \frac{1}{\sqrt{p}}(1, \dots, 1)$ is the normalized positive eigenvector of L corresponding to the zero eigenvalue. A linear transformation $\boldsymbol{u} := \boldsymbol{u}(\tau) = Q\boldsymbol{v}(\tau)$ yields

$$\boldsymbol{v}^T L\boldsymbol{v} = \boldsymbol{v}^T Q^T \operatorname{diag}\{0, \lambda_2, \dots, \lambda_p\} Q\boldsymbol{v} = \boldsymbol{u}^T \operatorname{diag}\{0, \lambda_2, \dots, \lambda_p\}\boldsymbol{u} = \sum_{i=2}^{p} \lambda_i u_i^2 \le 0.$$

To prove the claim, now it remains to show that $u_2, \dots, u_p$ cannot be simultaneously zero. Suppose not, then for some positive τ_0 we have

$$\boldsymbol{u}^T(\tau_0) = (u_1(\tau_0), 0, \dots, 0) = (\pm 1, 0, \dots, 0)$$

due to the fact that

$$\boldsymbol{u}^T\boldsymbol{u} = \boldsymbol{v}^T Q^T Q\boldsymbol{v} = \boldsymbol{v}^T\boldsymbol{v} = 1.$$

It follows from $\boldsymbol{v}(\tau) = Q^T Q\boldsymbol{v}(\tau) = Q^T\boldsymbol{u}(\tau)$ that $\boldsymbol{v}(\tau_0) = Q^T\boldsymbol{u}(\tau_0) = u_1(\tau_0)\boldsymbol{q}_1^T = \boldsymbol{q}_1^T \gg 0$. Thus $(F - \mathcal{R}_0 V)\boldsymbol{v} = 0$ implies

$$0 = (F - \mathcal{R}_0(\tau_0)(D - \tau_0 L))\boldsymbol{v}(\tau_0) = (F - \mathcal{R}_0(\tau_0)(D - \tau_0 L))\boldsymbol{q}_1^T = (F - \mathcal{R}_0(\tau_0)D)\boldsymbol{q}_1^T$$

and hence $\beta_i = \mathcal{R}_0(\tau_0)\gamma_i$, i.e., $\mathcal{R}_0(\tau_0) = \beta_i/\gamma_i$ for all i, a contradiction. Thus the claim holds.

It follows from $\boldsymbol{v}^T F\boldsymbol{v} > 0$ and $\boldsymbol{v}^T L\boldsymbol{v} < 0$ that

$$\frac{d\mathcal{R}_0}{d\tau} = (\mathcal{R}_0)^2 \frac{\boldsymbol{v}^T L\boldsymbol{v}}{\boldsymbol{v}^T F\boldsymbol{v}} < 0 \quad \text{for } \tau \in (0, \infty).$$

Therefore, $\mathcal{R}_0$ is a strictly decreasing function of τ on the interval $[0, \infty)$. ∎

Acknowledgments. The author sincerely thanks the two anonymous referees and the editor for their time and valuable comments, and Zhilan Feng, Jifa Jiang, Shigui Ruan, and Wendi Wang for helpful discussions.

REFERENCES

[1] L. J. S. Allen, B. M. Bolker, Y. Lou, and A. L. Nevai, *Asymptotic profiles of the steady states for an SIS epidemic patch model*, SIAM J. Appl. Math., 67 (2007), pp. 1283–1309, https://doi.org/10.1137/060672522.

[2] J. Arino, *Diseases in metapopulations*, in Modeling and Dynamics of Infectious Diseases, Z. Ma, Y. Zhou, and J. Wu, eds., Ser. Contemp. Appl. Math., Vol. 11, Higher Ed. Press, Beijing, 2009, pp. 64–122.

[3] J. Arino, A. Ducrot, and P. Zongo, *A metapopulation model for malaria with transmission-blocking partial immunity in hosts*, J. Math. Biol., 64 (2012), pp. 423–448.

[4] M. Bartlett, *Deterministic and stochastic models for recurrent epidemics*, in Proceedings of the Third Berkeley Symposium on Mathematical Statistics and Probability, Vol. 4, University of California Press, Berkeley, CA, 1956, pp. 81–109.

[5] C. Castillo-Chavez and H. Thieme, *Asymptotically autonomous epidemic models*, in Mathematical Population Dynamics: Analysis of Heterogeneity, Vol. 1, Theory of Epidemics, O. Arino, D. Axelrod, M. Kimmel, and M. Langlais, eds., Wuerz, Winnipeg, Canada, 1995, pp. 33–50.

[6] J. Chen and N. Xiao, *Chinese action towards global malaria eradication*, Lancet, 388 (2016), 959.

[7] J. Chen, L. Zou, Z. Jin, and S. Ruan, *Modeling the geographic spread of rabies in China*, PLoS Negl. Trop. Dis., 9 (2015), e0003772.

[8] C. Cosner, J. C. Beier, R. Cantrell, D. Impoinvil, L. Kapitanski, M. Potts, A. Troyo, and S. Ruan, *The effects of human movement on the persistence of vector-borne diseases*, J. Theor. Biol., 258 (2009), pp. 550–560.

[9] J. Cui, Y. Takeuchi, and Y. Saito, *Spreading disease with transport-related infection*, J. Theor. Biol., 239 (2006), pp. 376–390.

[10] J. M. Denstadli, *Analyzing air travel: a comparison of different survey methods and data collection procedures*, J. Travel Res., 39 (2000), pp. 4–10.

[11] O. Diekmann, J. A. P. Heesterbeek, and J. A. Metz, *On the definition and the computation of the basic reproduction ratio R_0 in models for infectious diseases in heterogeneous populations*, J. Math. Biol., 28 (1990), pp. 365–382.

[12] C. Dye and G. Hasibeder, *Population dynamics of mosquito-borne disease: effects of flies which bite some people more frequently than others*, Trans. R. Soc. Trop. Med. Hyg., 80 (1986), pp. 69–77.

[13] M. C. Eisenberg, Z. Shuai, J. H. Tien, and P. van den Driessche, *A cholera model in a patchy environment with water and human movement*, Math. Biosci., 246 (2013), pp. 105–112.

[14] G. R. Fulford, M. G. Roberts, and J. A. P. Heesterbeek, *The metapopulation dynamics of an infectious disease: tuberculosis in possums*, Theor. Popul. Biol., 61 (2002), pp. 15–29.

[15] D. Gao, C. Cosner, R. S. Cantrell, J. C. Beier, and S. Ruan, *Modeling the spatial spread of Rift Valley fever in Egypt*, Bull. Math. Biol., 75 (2013), pp. 523–542.

[16] D. Gao and C.-P. Dong, *Fast Diffusion Inhibits Disease Outbreaks*, preprint, https://arxiv.org/abs/1907.12229, 2019.

[17] D. Gao, Y. Lou, and S. Ruan, *A periodic Ross-Macdonald model in a patchy environment*, Discrete Contin. Dyn. Syst. Ser. B, 19 (2014), pp. 3133–3145.

[18] D. Gao and S. Ruan, *An SIS patch model with variable transmission coefficients*, Math. Biosci., 232 (2011), pp. 110–115.

[19] D. Gao and S. Ruan, *A multipatch malaria model with logistic growth populations*, SIAM J. Appl. Math., 72 (2012), pp. 819–841, https://doi.org/10.1137/110850761.

[20] D. Gao and S. Ruan, *Malaria models with spatial effects*, in Analyzing and Modeling Spatial and Temporal Dynamics of Infectious Diseases, D. Chen, B. Moulin, and J. Wu, eds., John Wiley & Sons, New York, 2014, pp. 109–136.

[21] J. W. Glasser, Z. Feng, S. B. Omer, P. J. Smith, and L. E. Rodewald, *The effect of heterogeneity in uptake of the measles, mumps, and rubella vaccine on the potential for outbreaks of measles: a modelling study*, Lancet. Infect. Dis., 16 (2016), pp. 599–605.

[22] G. Hasibeder and C. Dye, *Population dynamics of mosquito-borne disease: persistence in a completely heterogeneous environment*, Theor. Popul. Biol., 33 (1988), pp. 31–53.

[23] T. D. Hollingsworth, N. M. Ferguson, and R. M. Anderson, *Frequent travelers and rate of spread of epidemics*, Emerg. Infect. Dis., 13 (2007), pp. 1288–1294.

[24] Y.-H. Hsieh, P. van den Driessche, and L. Wang, *Impact of travel between patches for spatial spread of disease*, Bull. Math. Biol., 69 (2007), pp. 1355–1375.

[25] J. M. Hyman and T. LaForce, *Modeling the spread of influenza among cities*, in Bioterrorism: Mathematical Modeling Applications in Homeland Security, H. Banks and C. Castillo-Chavez, eds., SIAM, Philadelphia, 2003, pp. 215–240, https://doi.org/10.1137/1.9780898717518.ch10.

[26] International Union of Railways, *High Speed Lines in the World (summary)*, 2019, https://uic.org/IMG/pdf/20190328_high_speed_lines_in_the_world.pdf.

[27] J. Jiang, *On the global stability of cooperative systems*, Bull. Lond. Math. Soc., 26 (1994), pp. 455–458.

[28] Y. Jin and W. Wang, *The effect of population dispersal on the spread of a disease*, J. Math. Anal. Appl., 308 (2005), pp. 343–364.

[29] R. Liu, J. Shuai, J. Wu, and H. Zhu, *Modeling spatial spread of West Nile virus and impact of directional dispersal of birds*, Math. Biosci. Eng., 3 (2006), pp. 145–160.

[30] X. Liu and Y. Takeuchi, *Spread of disease with transport-related infection and entry screening*, J. Theor. Biol., 242 (2006), pp. 517–528.

[31] Office of Highway Policy Information, *State motor-vehicle registrations*—2015, 2017, https://www.fhwa.dot.gov/policyinformation/statistics/2015/mv1.cfm.

[32] S. Ruan, W. Wang, and S. A. Levin, *The effect of global travel on the spread of SARS*, Math. Biosci. Eng., 3 (2006), pp. 205–218.

[33] L. A. Rvachev and I. M. Longini, Jr., *A mathematical model for the global spread of influenza*, Math. Biosci., 75 (1985), pp. 3–22.

[34] M. Salmani and P. van den Driessche, *A model for disease transmission in a patchy environment*, Discrete Contin. Dyn. Syst. Ser. B, 6 (2006), pp. 185–202.

[35] A. Santos, N. McGuckin, H. Y. Nakamoto, D. Gray, and S. Liss, *Summary of travel trends: 2009 national household travel survey*, 2011, https://nhts.ornl.gov/2009/pub/stt.pdf.
[36] H. L. Smith, *Monotone Dynamical Systems: An Introduction to the Theory of Competitive and Cooperative Systems*, Math. Surveys Monogr. Vol. 41, AMS, Providence, RI, 1995.
[37] J. Sullivan, K. Kershaw, and J. Cummings, *National Travel Survey: England* 2015, 2016, https://www.gov.uk/government/statistics/national-travel-survey-2015.
[38] C. Sun, W. Yang, J. Arino, and K. Khan, *Effect of media-induced social distancing on disease transmission in a two patch setting*, Math. Biosci., 230 (2011), pp. 87–95.
[39] A. J. Tatem, D. J. Rogers, and S. I. Hay, *Global transport networks and infectious disease spread*, Adv. Parasitol., 62 (2006), pp. 293–343.
[40] The World Bank Group, *Air transport, passengers carried*, 2018, https://data.worldbank.org/indicator/IS.AIR.PSGR.
[41] R. B. Turner, *The epidemiology, pathogenesis, and treatment of the common cold*, Semin. Pediatr. Infect. Dis., 6 (1995), pp. 57–61.
[42] R. B. Turner, *Epidemiology, pathogenesis, and treatment of the common cold*, Ann. Allergy Asthma Immunol., 78 (1997), pp. 531–540.
[43] P. van den Driessche and J. Watmough, *Reproduction numbers and sub-threshold endemic equilibria for compartmental models of disease transmission*, Math. Biosci., 180 (2002), pp. 29–48.
[44] W. Wang, *Epidemic models with population dispersal*, in Mathematics for Life Science and Medicine, Y. Takeuchi, Y. Iwasa, and K. Sato, eds., Springer, Berlin, 2007, pp. 67–95.
[45] W. Wang and G. Mulone, *Threshold of disease transmission in a patch environment*, J. Math. Anal. Appl., 285 (2003), pp. 321–335.
[46] W. Wang and X.-Q. Zhao, *An epidemic model in a patchy environment*, Math. Biosci., 190 (2004), pp. 97–112.
[47] X. Wang, S. Liu, L. Wang, and W. Zhang, *An epidemic patchy model with entry–exit screening*, Bull. Math. Biol., 77 (2015), pp. 1237–1255.
[48] World Health Organization, *Pandemic (H1N1) 2009—update* 60, 2009, https://www.who.int/csr/don/2009_08_04/en/.
[49] World Health Organization, *Zika situation report—28 July* 2016, 2016, https://www.who.int/emergencies/zika-virus/situation-report/28-july-2016/en/.
[50] L. Xue, H. M. Scott, L. W. Cohnstaedt, and C. Scoglio, *A network-based meta-population approach to model Rift Valley fever epidemics*, J. Theor. Biol., 306 (2012), pp. 129–144.
[51] J. Zhang, Z. Jin, and H. Zhu, *Birds movement impact on the transmission of West Nile virus between patches*, J. Appl. Anal. Comput., 8 (2018), pp. 443–456.
[52] X.-Q. Zhao, *Dynamical Systems in Population Biology*, 2nd ed., Springer, Cham, 2017.
[53] X.-Q. Zhao and Z.-J. Jing, *Global asymptotic behavior in some cooperative systems of functional differential equations*, Canad. Appl. Math. Quart., 4 (1996), pp. 421–444.